International Journal of Nanomedicine

Dovepress
open access to scientific and medical research

Open Access Full Text Article

ORIGINAL RESEARCH

Presence of Titanium and Toxic Effects Observed in Rat Lungs, Kidneys, and Central Nervous System in vivo and in Cultured Astrocytes in vitro on Exposure by Titanium Dioxide Nanorods

This article was published in the following Dove Press journal:
International Journal of Nanomedicine

András Papp[1]
Tamara Horváth[1]
Nóra Igaz[2]
Mohana Krishna Gopisetty[2]
Mónika Kiricsi[2]
Dániel Simon Berkesi[3]
Gábor Kozma[3]
Zoltán Kónya[3]
Imola Wilhelm[4]
Roland Patai[4]
Tamás Ferenc Polgár[4]
Tamás Bellák[5]
László Tiszlavicz[6]
Zsolt Razga[6]
Tünde Vezér[1]

[1]Department of Public Health, Faculty of Medicine, University of Szeged, Szeged, Hungary; [2]Department of Biochemistry and Molecular Biology, Faculty of Science and Informatics, University of Szeged, Szeged, Hungary; [3]Department of Applied and Environmental Chemistry, Faculty of Science and Informatics, University of Szeged, Szeged, Hungary; [4]Institute of Biophysics, Biological Research Centre, Szeged, Szeged, Hungary; [5]Department of Anatomy, Histology and Embryology, Faculty of Medicine, University of Szeged, Szeged, Hungary; [6]Department of Pathology, Faculty of Medicine, University of Szeged, Szeged, Hungary

Background: Non-spherical titanium dioxide (TiO_2) nanoparticles have been increasingly applied in various biomedical and technological fields. Their toxicological characterization is, however, less complete than that of roundish nanoparticles.

Materials and Methods: Anatase form TiO_2 nanorods, ca. 15x65 nm in size, were applied to cultured astrocytes in vitro and to the airways of young adult Wistar rats in vivo in 5, 10, and 8 mg/kg BW dose for altogether 28 days. Presence of nanorods and cellular damage was investigated in the astrocytes and in rat lungs and kidneys. Functional damage of the nervous system was studied by electrophysiological methods.

Results: The treated astrocytes showed loss of viability without detectable apoptosis. In rats, TiO_2 nanorods applied to the airways reached the blood and various organs including the lungs, kidneys, and the central nervous system. In lung and kidney samples, nanorods were observed within (partly damaged) phagolysosomes and attached to organelles, and apoptotic cell death was also detected. In cortical and peripheral electrophysiological activity, alterations corresponding to energy shortage (resulting possibly from mitochondrial damage) and astrocytic dysfunction were detected. Local titanium levels and relative weight of the investigated organs, apoptotic cell death in the lungs and kidneys, and changes in the central and peripheral nervous activity were mostly proportional to the applied doses, and viability loss of the cultured astrocytes was also dose-dependent, suggesting causal relationship of treatments and effects.

Conclusion: Based on localization of the visualized nanorods, on neuro-functional changes, and on literature data, the toxic mechanism involved mitochondrial damage, oxidative stress, and apoptotic cell death. These indicate potential human toxicity and occupational risk in case of exposure to rod-shaped TiO_2 nanoparticles.

Keywords: apoptosis, nanoparticles, neuro-functional changes, tissue damage, toxicity

Introduction

Titanium dioxide nanoparticles (TiO_2 NPs) of various shape and size are currently found in numerous applications. This involves possible human exposure in occupational settings (during manufacturing and processing of the nanomaterial) and via certain consumers' goods (eg, sunscreens or accidental presence of NPs in pigment-grade TiO_2 powder used in food and drugs).[1]

One of the major technical advantages of nano-TiO_2 is spontaneous or photocatalytic oxidative action, which is utilized among others in self-cleaning, self-

Correspondence: András Papp
Department of Public Health, Faculty of Medicine, University of Szeged, Dóm Tér 10, H-6720, Szeged, Hungary
Tel +36 62 342870
Fax +36 62 545120
Email papp.andras@med.u-szeged.hu

submit your manuscript | www.dovepress.com
DovePress
http://doi.org/10.2147/IJN.S275937

sanitizing surfaces, and antimicrobial treatment of textile items.[2,3] For some of such applications, non-spherical, elongated NPs have been found preferable.[4] On the other hand, oxidative activity is a source of risk when TiO_2 NPs come into interaction with living organisms including humans.

A general property of NPs is that they cause redox imbalance and oxidative stress in cells, resulting from their high surface-to-volume ratio (a parameter influenced also by the NPs' shape) and from surface characteristics such as defects of crystal structure, surface atoms with free valence electrons, and adsorbed redox active metal ions.[5,6] In the aqueous microenvironment of living tissues, the reactive oxygen species (ROS) generated as a result of the NPs' surface activity will damage biomolecules if antioxidant capacity of the cells is insufficient.[7] Organs of high energy demand, such as the brain or the kidneys, show special sensitivity to oxidative stress because of their intense mitochondrial activity.[8,9] Oxidative stress in the brain evoked by TiO_2 NP exposure has been repeatedly reported in the literature.[10] Renal oxidative stress and cell death in TiO_2 NP treated animals have also been described.[11]

The above mentioned widespread application and the properties of TiO_2 NPs have led to concerns about their possible health effects.[12] The most likely form of TiO_2 (and other) NPs in the environment is nano-aerosol in the air. Consequently, a significant part of human exposure to nano-TiO_2 is via the airways, resulting in possible damage both locally in the lungs and in distant organs via blood and lymphatic flow. Occupational exposure by airborne nano-TiO_2 was associated with oxidative stress, inflammation, and lung damage, indicated by the workers' serum biomarkers.[13] In rats, a single inhaled dose of several sizes of anatase TiO_2 NPs induced an increase in various cytokines and cytotoxicity markers in the lungs; the strongest effect was seen in case of 10–30 nm spherical particles.[14] In one of our previous studies, rod-shaped TiO_2 NPs induced several inflammatory cytokines in the lungs of rats exposed to the nanorods subacutely via the airways.[15]

The kidneys, exerting the function of removing xenobiotics, showed oxidative stress, increased inflammation markers, as well as functional and histological damages due to tubular necrosis in rats treated orally with (unspecified) nano-TiO_2.[16] In another study, lipid peroxidation, reduced antioxidant activity, and proximal tubular apoptosis has been observed in the kidneys of rats after oral administration of spherical TiO_2 NPs of <100 nm in size for 3 weeks.[17]

Inhaled NPs can reach the brain by crossing the alveolar and blood–brain barriers (BBB) or by migrating along olfactory and other afferent nerve fibers.[18] The vagus nerve, innervating large sections of the respiratory and digestive tracts, can convey both inhaled and ingested NPs up to the brainstem.[19]

The size and shape of NPs can be crucial in crossing barriers. Particles below 30–35 nm size were found to migrate from the alveoli to the bloodstream, whereas larger ones stayed on the epithelial surface.[20] A difference in penetration has been reported between approx. 30 nm in nanospheres and approx. 20x40 nm in nanorods of TiO_2 through modeled human BBB in vitro and to rat brain in vivo.[21] Furthermore, individual fibers of the olfactory nerve cannot forward particles above approx. 100 nm size.[22] On the other hand, barrier crossing of NPs is promoted by caveola formation[23] and endothelial weakening,[24] and the latter was also found to be size/shape dependent.[21]

In rats that inhaled an aerosol of 10 mg/m^3 nano-TiO_2 (20–25 nm spheres, mostly anatase) for 6 hours daily, 5 days a week for 4 weeks, damage to the brain was indicated by an increased level of inflammation markers and a decreased expression of synaptophysin, but no deposition of titanium could be detected.[25] In another study, TiO_2 NPs (5–10 nm spheres, anatase) given to rats orally for 2 months caused lower acetylcholinesterase activity and higher glial fibrillary acidic protein (GFAP) reactivity and interleukin-6 (IL-6) levels in the brain.[26] In postmortem brain samples of persons exposed to NP-laden polluted urban air, protein markers of Alzheimer's and Parkinson's diseases were associated to the presence of Ti-rich NPs.[19] Exposure to titanium-based pigment particles in the workplace atmosphere has been reported to cause neurological symptoms.[27]

In contrast to molecular and biochemical studies, there is only a low number of papers describing TiO_2 NP-induced nervous system damage by means of electrophysiological recording.[10] In neuronal networks of mouse frontal cortex origin, which were cultured in vitro and treated with TiO_2 NPs (of 90–100 nm diameter, 10 µg/cm^2 culture area, 24 hours), uptake of the NPs into the cells and substantial decrease of discharge activity were observed.[28] In mice, neuronal degeneration and dose-dependent reduction of hippocampal long-term potentiation were observed in vivo, after a 90-day intranasal administration of suspended anatase TiO_2 NPs (ca. 300 nm agglomerates of 5–6 nm primary particles).[29] In one of our previous works performed in rats with subacute

intratracheal application of spherical anatase TiO_2 NPs, effects on cortical and peripheral electrophysiological phenomena indicating functional damage were observed, and these alterations had a clear relationship to Ti levels and oxidative stress detected in the blood and brain.[30]

Overwhelming oxidative stress at cellular level often leads to cell death. Alveolar macrophages isolated from rats following a single intratracheal instillation of TiO_2 NPs showed signs of oxidative stress and cytotoxicity, but the mechanism of cell death has not been clarified.[31] Cells of the HT22 mouse hippocampal neuronal line showed apoptosis with increased Ca^{2+} and ROS levels on exposure to TiO_2 nanospheres of approx. 50 nm size.[32] Additionally, in the majority of studies suggesting that nano-TiO_2 affects the human brain, results have been achieved by using in vitro models based on human nervous system derived cells. Mitochondrial damage, reduced growth, and NP internalization were described in neuronal and glial cell lines of human origin exposed to TiO_2 nanospheres of approx. 15 nm size.[33] In a cultured human-derived neuronal cell line (SH-SY5Y), internalized TiO_2 NPs of 25 nm of nominal size have been found to cause apoptosis and altered cell cycle but no oxidative stress.[34]

Besides the size and surface features, the shape of the NPs determines their suitability for various technical applications. In several cases, elongated particles, such as nanorods, nanotubes, or nanowires, have been proven to be more advantageous than the spherical/isometric ones, eg, in solar cells, drug delivery, or antimicrobial treatment of fabrics.[4,35,36] Nanorods used in boosting the immune function and surface nanostructures of dental and orthopedic implants (from which particles can be released due to wear) were in the same size range as the nanorods used in the present study.[37–39]

In spite of the actual or potential applications of non-spherical NPs outlined above, the majority of available literature focuses on effects (including toxicity) exerted on biological objects by TiO_2 nanospheres. Furthermore, most of the papers published on the action of TiO_2 NPs describe effects exerted on single organs, even if the literature suggests that events at (sub)cellular level, first of all, oxidative stress and apoptotic cell death, are universally present, and may be responsible for various alterations (morphological and/or functional) in different organs of nano-TiO_2 exposed experimental animals.

Based on the above findings and our previous results with spherical TiO_2 NPs, in the present study, rod-shaped TiO_2 NPs of 10–20x50–100 nm (diameter x length) size range were administered to the rats via the airways to obtain a realistic model of exposure to airborne NPs. In a multi-organ approach, the presence of the nanorods and the induced cell damage were studied in the treated rat lungs and kidneys, and the functional alterations of the nervous system were investigated by analyzing cortical, subcortical, and peripheral electrophysiological phenomena. Electrophysiological signs can be simply and non-invasively recorded in humans. They may provide the base of developing functional biomarkers of toxicity, provided that the relationship of toxic exposure, eg, to nano-TiO_2, and electrophysiological alterations are described. The effects on cultured astrocytes, a cell type fulfilling several essential roles in the functioning of the brain, were examined in vitro. We assessed the pathomorphological effects (cellular and subcellular signs of cytotoxicity induced in different organs by the nanorods) and changes of the nervous electrophysiological activity, concerning the extent to which they were similar to or different from those which have been described with NPs of other size and shape.

Materials and Methods

Manufacturing and Characterization of Nanorods

Using a simple alkali hydrothermal method, Degussa P25 TiO_2 nano-powder (Sigma-Aldrich, St. Louis, PA, USA) was processed first to nanotubes as intermediate products, and finally, to nanorods of TiO_2 with approx. 15x65 nm size and of anatase crystal structure.[40] The particle size was checked by X-ray diffraction in dry state and by transmission electron microscopy (TEM) and dynamic light scattering (DLS) after suspending the nanomaterial in the application medium (phosphate-buffered saline at pH 7.0 with 1% polyacrylic acid (PAA) added for suspension stability). The crystal structure of the nanorods was predominantly anatase, which is known to have higher chemical activity (including ROS generation).[41] TEM and DLS were performed both on freshly made suspension and after 3 months of storage at room temperature to prove suspension stability. Details of preparation of the TiO_2 NPs and the suspension, and the characteristics of them, were published by Horváth et al.[15]

In vitro Investigations

Isolation and Culture of Primary Mouse Astrocytes

Astrocytes were isolated from the brain of 1-day-old mouse pups (strain: BALB/cAnNCrl, Charles River Laboratories, USA; the SPF breeding stock was kept

under standard conditions in the Central Animal House of the Biological Research Center) by mechanical dissociation. After passing through a 40 µm pore-size strainer (Corning Inc., Corning, NY, USA), the collected cells were seeded onto poly-L-lysine-coated dishes and kept in a CO_2 incubator (5% CO_2, 37°C, 85–95% humidity) in low-glucose Dulbecco's Modified Eagle Medium (DMEM; Thermo Fisher Scientific, Waltham, MA, USA) supplemented with 10% fetal bovine serum (FBS; Merck-Sigma, St. Louis, MO, USA). The medium was replaced twice a week. The cell layer reached confluency after 2 weeks, and the cultures were subsequently used for the experiments.

Cell Viability Test

The effect of TiO_2 NPs on the viability of the primary mouse astrocytes was tested by MTT assay after adding the nanosuspension to the culture medium in final concentrations ranging from 0.05 to 2.00 mg/mL for 24 and 48 hours. In parallel, the action of the corresponding amounts of 1% PAA-containing vehicle was tested on astrocytes as well. Following the treatments, the astrocytes were rinsed with PBS and incubated in a culture medium with the addition of 0.5 mg/mL MTT reagent (Serva, Heidelberg, Germany) for 1 h at 37°C. Formazan crystals generated by the living cells were solubilized in 100 µL DMSO. The absorbance was measured at 570 nm with a Synergy HTX plate reader (BioTek, Winooski, VT, USA). MTT measurements were repeated three times, using at least three independent biological replicates.

Apoptosis Detection by Means of Annexin V–Propidium Iodide Staining

Apoptosis induced in the cultured astrocytes after exposure to TiO_2 nanorods was examined by Annexin V and propidium iodide (PI) staining. The 2-week-old cultures were treated either with 0.1 mg/mL TiO_2 NPs or with the corresponding dose of PAA for 24 hours. Then, the cells were stained with Alexa488-conjugated Annexin V and with PI as described in the manufacturer's guideline (Thermo Fisher Scientific, Waltham, MA, USA). The intensity of fluorescence was measured by a FACSCalibur flow cytometer (BD, Franklin Lakes, NJ, USA) on 10,000 cells, and the FACS data were analyzed by the FlowJo V10 software. The detection of apoptosis was repeated three times using at least two biological replicates.

Detection of TiO_2 Nanorods in the Cultured Astrocytes by Means of Scanning Electron Microscopy and Energy Dispersive X-Ray Spectroscopy

For this investigation, the freshly isolated cells were seeded onto plastic cover slips (Sarstedt, Nümbrecht, Germany) positioned in the wells of standard 6-well plates, and were cultured for 2 weeks as described above. Then, the cells were treated with 0.1 mg/mL TiO_2 NPs for 24 hours, rinsed, and fixed by means of 2.5% glutaraldehyde (dissolved in modified Sörensen buffer, pH 7.6). Dehydration was done in an ascending ethanol series, and then, in a series of tert-butanol/ethanol mixture at room temperature. After that, the cells were incubated in tert-butanol overnight at 4°C, and finally, lyophilized. The cover slips were fixed on specimen stubs by an electrically conductive double-sided adhesive tape, and a gold-palladium layer of 4–5 nm was applied to reduce charging artefacts and radiation damage to the sample. Scanning electron microscopic (SEM) images were obtained using a Hitachi S4700 electron microscope (Hitachi High-Technologies Europe GmbH, Krefeld, Germany) with accelerating voltage and emission current set to 10 kV and 10 µA, respectively. The presence of Ti was verified by energy dispersive spectroscopy (EDS) by means of a Röntec QX2 EDS detector mounted on the SEM with 10 kV and 10 µA at multiple points from the cells with attached, visually identified NPs and also from the background. The presence of Ti was confirmed based on the Kα peak of the element at 4.508 keV.

In vivo Investigations

Animals and Housing

Young adult male SPF Crl:WIBr Wistar rats (6 weeks old, 170±20 g body weight), altogether 50 animals, were obtained from Toxi-Coop Ltd (Budapest, Hungary). They were housed in an animal facility providing good laboratory practice-equivalent conditions (two animals per cage, 12–12-hour light/dark cycle with light on at 06:00; temperature 22±3°C, relative humidity 30–70%). Access to standard rodent food (Ssniff R/M-Z+H, Toxi-Coop Ltd) and tap water was unlimited. The rats were acclimated for 1 week, and then randomized to 5 treatment groups of 10 rats each.

During the whole study, the principles of the Ethics Committee for the Protection of Animals in Research of the University of Szeged were strictly followed. The study was approved by the authority competent in animal welfare issues (License No. XXI/151/2013 issued by the

Csongrád County Government Office, Directorate for Food Chain Safety).

Treatment

The treatment of the five groups was the following: The control group (C) was given saline. The vehicle treated (VT) group received the suspension medium of the NPs, and the treated groups (LD, MD, HD) were given TiO_2 nanorods suspended in the vehicle. The rats received the corresponding treatment by intratracheal instillation of 1 mL/kg BW volume, performed in brief anesthesia once daily, 5 days per week, altogether 28 times over a 6-week period, always between 8:00 am and 10:00 am as described in.[42] Before application, the nano-TiO_2 suspension was sonicated to counteract aggregation. Table 1 shows the coding and treatment of each group. The doses applied were identical to those used in a previous work on nano-TiO_2 nanorods effects on rats lungs,[15] with the aim of generalizing the earlier findings this time to a more complex approach.

General Toxicology: Investigation of Weight Gain and Clinical Symptoms

The body weight (as a parameter of general toxicity) of the rats was measured every treatment day, in the morning before administration of the substances, to assess the appropriate amount to be instilled. The effect of nano-TiO_2 dependent toxicity on growth was investigated on the basis of body weight measured at equal 7-day intervals (Monday to Monday). The resulting growth rate was analyzed in relation to doses and the age of the rats (increasing with the treatment weeks). Visible clinical symptoms (eg, rough fur or unusual behavior) or death, indicating general toxicity, were also observed and registered daily.

Investigation of Central and Peripheral Electrophysiological Activities

On the day following the last treatment, the rats were prepared for electrophysiological recording and tissue sampling in terminal anesthesia using urethane (Molar, Budapest, Hungary) in 1000 mg/kg BW dose given intraperitoneally.[43] Hind leg withdrawal reflex was used to assess the depth of anesthesia.[44]

The parietal bone above the left hemisphere was removed, and the dura was protected from drying by a thin layer of white petrolatum (for details of preparation, see).[42] The prepared rats were covered in a warm cloth to maintain body temperature and were allowed to recover for at least 30 min before recording.

The head of the rat was fixed for recording in the stereotaxic frame of the electrophysiological setup. A thermostated (+36.5°C) base plate provided support to the rat's underside and body temperature stabilization during recording. Recording electrodes (silver wire, ball-tipped) were placed on the dura over the primary somatosensory (SS) projection area of the whisker pad and over the primary visual (VIS) and auditory (AUD) focuses. The sites were located with the aid of a somatotopic map,[45] and the electrodes were fine positioned by finding the punctum maximum of the evoked response. A stainless steel clamp was attached to the cut skin edge as indifferent electrode.

Spontaneous electrical activity (electrocorticogram, ECoG) was taken from the three sites for 6 min. From that, the relative spectral power of the frequency bands (delta, theta, alpha, beta1, beta2, and gamma; standard human EEG bands)[46] was automatically determined. The "ECoG index" (a handy, albeit simplifying descriptor of the ECoG spectrum)[47] was calculated from the relative band powers as: ([delta]+[theta])/([beta1]+[beta2]).

Then, sensory evoked potentials (EPs) were elicited and recorded. SS stimuli were square electric pulses (3−4 V; 0.05 ms) delivered through a pair of needles inserted into the contralateral whisker pad. VIS stimulation was performed by flashes of a white high-luminescence LED directed into the rat's contralateral eye. For AUD stimulation,

Table 1 Groups of Rats Used in the in vivo Work with Their Coding and Treatment

Group	Code	Substance	Dose	Volume
Control	C	Normal saline (NaCl 0.9%)	—	1 mL/kg BW
Vehicle treated	VT	Phosphate buffered saline with 1% PAA	—	
Low dose treated Medium dose treated High dose treated	LD MD HD	TiO_2 nanorods suspended in the vehicle	5 mg/kg BW 10 mg/kg BW 18 mg/kg BW	

Abbreviations: BW, body weight; PAA, polyacrylic acid.

clicks (approx. 40 dB) were applied into the contralateral ear of the rat from a mini earphone through the hollow ear bar of the stereotaxic frame. In each modality, one series of 50 stimuli was applied with 1 Hz frequency, and the onset latency of the recorded EPs was measured after averaging (for details of measuring, see Supplementary Figure 1). It has been described in previous studies that the dynamic interaction of successive excitation processes in a sensory pathway, a phenomenon reflecting the actual state of the CNS, can be examined by varying the frequency of stimulation.[48] Hence, SS EPs were also recorded using one series of stimuli with 2 and 10 Hz frequency beyond the standard 1 Hz.

Based on the observed effects of nano-TiO_2 on motor behavior,[49] it was examined if the connection between the motor cortical area and the caudato-putamen was influenced by the treatment. The cortex was stimulated by applying the stimulus trains of 50 described above, at 1 Hz frequency, via a bipolar electrode. Evoked activity of the caudate-putamen (CPu) was led off with a steel needle electrode (stereotaxic coordinates: cortical site; AP −1, L 2; CPu; AP 0, L 3, V −5).[45] The biphasic responses obtained from the CPu were evaluated the same way as the cortical EPs.

The recording session was ended with obtaining compound action potentials (CAP) of the tail nerve. A pair of stimulating needle electrodes were inserted at the base of the tail (delivering similar electric stimuli to the ones used for whisker stimulation), and the CAPs were recorded 50 mm distally by another pair of needles. From the onset latency of the CAP and the distance of the electrodes, conduction velocity of the tail nerve was obtained. The relative refractory period of the tail nerve was calculated by double-pulse stimulation, from the ratio of the latency of the second and first CAP at different interstimulus intervals. The complete recording and evaluation was performed by means of the NEUROSYS 1.11 software (Experimetria Ltd, Budapest, Hungary).

Complex Post-Mortem Investigation: Further General Toxicological and Chemical (A), Biochemical (B), and Pathomorphological (C) Examinations

Investigation A – Relative Organ Weights and Ti-Levels of Tissues

When the electrophysiological recording was finished, the rats were sacrificed with overdosed urethane (two-fold of the anesthetic dose secured gentle and quick sacrifice). After the last breath, necropsy started with opening the thorax and taking 3–4 mL blood from the left ventricle for the measurement of Ti concentration. Then, the rats were perfused transcardially with 300 mL cooled saline (4°C) to rinse blood from the organs and were dissected.

The brain (complete with both hemispheres and cerebellum) was removed, weighed, shock-frozen in liquid nitrogen, and stored at –20°C. The lungs, hilar lymph nodes, thymus, heart, liver, spleen, kidneys, and adrenals were removed and weighed. The right half of the lung and the right kidney were shock-frozen and stored as above, while the left lung and kidney and the lymph nodes were fixed in 4% neutral buffered formalin for pathological investigation (see below). The relative organ weights (related to 1/100 body weight and to brain weight) were obtained for all the listed organs.

The level of titanium in the frozen blood, brain, lung, and kidney samples was determined by single-particle inductively coupled plasma mass spectrometry (ICP-MS; quadrupole 7700x; Agilent, Santa Clara, CA, USA). The samples were processed for ICP-MS measurement as described earlier.[15,30] The liquid obtained was filtered on 0.45 nm hydrophilic membrane filter and diluted to 100 mL final volume.

Investigation B – Oxidative Tissue Damage

In the lung samples, the extent of oxidative damage was assessed by measuring lipid peroxidation (thiobarbiturate reaction, TBARS) and catalase activity, using lysates of freeze-dried lung tissue. Lipid peroxidation was measured as μM malondialdehyde/mg protein, and catalase activity, in "Bergmeyer units" (BU/mg protein). For details, see Ref. 15.

Investigation C – Light and Electron Microscopy and Immunohistochemistry

In the samples of the lungs and of renal cortex and medulla, pathomorphological alterations were investigated by light and electron microscopy. For light microscopy (LM), slices of 3 μm thickness were made of formalin-fixed and paraffin-embedded tissue blocks, and were stained by hematoxylin-eosin (HE) for observing abnormalities at cellular level such as macrophages laden with NPs or signs of cell injuries (necrosis, apoptosis, or autophagy).

TiO_2 NPs were identified and their relationship to subcellular components and the damage caused in them were determined by TEM and EDS. Tissue blocks were deparaffinated and re-embedded in epoxy resin (Embed 812; Sigma-Aldrich, St. Louis, PA, USA) using a routine TEM sample preparation protocol. Ultrathin slices of 70

nm thickness were cut, stained with uranyl acetate and lead citrate, and placed on standard copper grids. The samples were analyzed in a JEM-1400Flash transmission electron microscope (JEOL; Tokyo, Japan).

First, the sections were systematically screened at low magnification (1000–5000×) to find NPs. To identify these as TiO_2 NPs by means of EDS, the sections were examined at 80,000–120,000× magnification with the EM-14620SIOD scanning transmission detector (JEOL) operated at 120 kV acceleration voltage. A Dry SD30GV SDD 30 mm^2 X-ray detector (JEOL) was used for the electron probe X-ray microanalysis. Although this method is seldom used on tissue specimens, it is regarded as highly accurate and reliable.[50]

The X-ray spectra were recorded in the 0–40 keV energy range for 100 seconds live time and were analyzed by the Visual Identification- and Thin Film Standardless Quantitative Analysis Program of the JED-2300 Analysis Station (JEOL). The characteristic X-ray fingerprint of titanium was identified by its Kα transition line at 4.508 keV.

To what extent the cell damage, observed by light and electron microscopy, corresponded to apoptosis was examined by the TUNEL (terminal deoxynucleotidyl transferase dUTP nick end labeling) assay. Lung and kidney sections cut to 8 µm from paraffin-embedded blocks were laid on silanized slides, stained with Click-iT Plus TUNEL Assay using Alexa Fluor 488 dye (C10617; Invitrogen, Carlsbad, CA, USA) and counterstained with DAPI (4′,6-diamidino-2-phenylindole; Sigma D9542; Sigma-Aldrich, St. Louis, PA, USA) following the manufacturer's instructions. The sections were covered with Vectashield mounting medium (H-1000-10, Vector Laboratories, Inc., Burlingame, CA, USA). Microphotographs were taken with an Olympus Fv10i-W compact confocal microscope system (Olympus) with Fv10i software (V2.1; Olympus Ltd, Tokyo, Japan) at 60x magnification (NA: 1.35). For counting the apoptotic and total (DAPI-stained) number of nuclei of the cells, Cell Counter plugin of the NIH ImageJ analysis software was used (imagej.nih.gov/ij). Control (n=3), vehicle-treated (n=3), low dose (n=6), medium dose (n=6), and high dose (n=6) treated animals were analyzed. Apoptosis was quantified in five randomly selected images per animal (technical replicates); data were expressed as percentage of TUNEL+/DAPI ratio and averaged for each animal (biological replicates). Representative images were further processed with the GNU Image Manipulation Program (GIMP 2.10.10; gimp.org).

Statistics

Individual data were processed to group means and standard deviation (SD). Normality of data distribution was checked by the Kolmogorov–Smirnov test. In case of sufficiently normal distribution, one-way ANOVA (for organ weight and 24-hour astrocyte viability) and general linear model (GLM) with repeated measures (for body weight and body weight growth rate) main tests and post hoc Tukey's test were used. In case of non-normal distribution of data, non-parametric Kruskal–Wallis ANOVA and post hoc Mann–Whitney *U*-test with Holm correction was applied (for electrophysiological, chemical, biochemical data, and 48-hour astrocyte viability). The significance limit of was set at $p<0.05$ for each test. SPSS version 24.0 (IBM, Armonk, NY, USA) and RStudio version 3.6.1 (for the TUNEL test; RStudio, Inc., Boston, MA, USA) were used. Linear correlation between data sets was searched for by means of the "linear fit" function in MS Excel (which applies the least square method to fit a straight line to the measurement data and tests the strength of relationship with Fisher's *F*-test).

Results

In vitro Effects on the Cultured Astrocytes

Presence of TiO_2 NPs

The presence of the nanorods on the surface of the cultured astrocytes, in vitro representatives of the nervous tissue, was directly confirmed by means of SEM-EDS. In Figure 1, NPs are visualized on the surface of a cultured astrocyte, and the EDS spectrum obtained from that spot (but not from a background spot) shows the presence of Ti (Kα transition line at 4.508 keV).

Effect of the TiO_2 Nanorods on the Astrocytes

The treatment of the cultured astrocytes with various concentrations of TiO_2 NP resulted in dose-dependent loss of viability. As seen in Figure 2, cell viability decreased monotonously with the increasing doses of nano-TiO_2. At higher doses, treatment with the vehicle had some effect, but that was mild and clearly distinguishable from the cytotoxicity of the nanorods. The higher nano-TiO_2 doses had stronger effect after 48 hours than after 24 hours, but the calculated IC_{50} was nearly identical (24 hours: IC_{50}=612.1 µg/mL; 48 hours: IC_{50}=610.4 µg/mL).

In spite of the viability loss, no apoptosis (shown by the similarity of cell numbers in the Q2 and Q3 quadrants in control and treated samples) and no necrosis (shown by the similarity of cell numbers in the Q1 quadrant) were

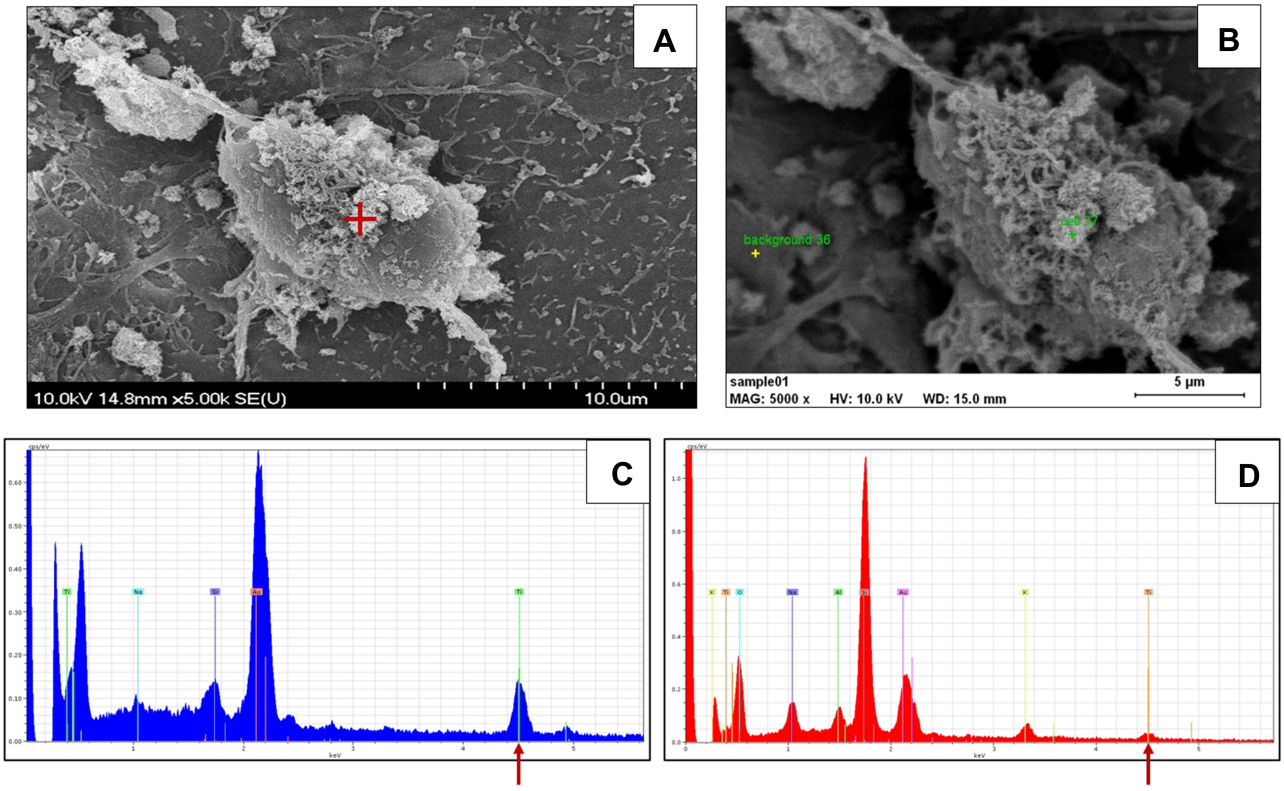

Figure 1 Presence of titanium in treated astrocytes. (**A**) Scanning electron micrograph of an astrocyte with cell-attached NPs (red cross). (**B**) Sites of energy dispersive spectroscopic sampling indicated at the NPs and at a background spot. (**C**) EDS spectrum taken from the site marked with red cross in A, showing massive presence of Ti (Kα peak at 4.508 nm, arrow). (**D**) EDS spectrum taken from a background site where the presence of Ti was minimal.
Abbreviations: EDS, energy dispersive spectroscopy; NP, nanoparticle; Ti, titanium.

detected in the treated cultures by means of the Annexin V–propidium iodide staining method (Figure 2C). All the same, dose dependence of the viability loss of the treated astrocytes and the verified presence of Ti-containing NPs on them underlined the causal relationship between the two.

In vivo Effects Observed in the Treated Rats

Presence of Chemically Detected Ti in the Rats' Tissue Samples

Among the treated rats, first of all in group HD, the level of Ti detected by ICP-MS was elevated vs both C and VT. In the lungs, the increase was highly significant, and it was also significant in the kidneys and in the liver (Supplementary Figure 2). In the brain and blood samples, the increase was moderate and remained below significance.

General Toxic Effects Observed in the Rats

Treatment on altogether 28 days with the anatase TiO_2 nanorods caused no clinical signs in the treated animals compared to the control ones. During daily routine handling, no death, no external abnormalities (such as rough fur), and no unusual behavior, motion, or posture was observed in the treated rats.

There was no noteworthy effect on body weight gain as shown by the data in Supplementary Figure 3. There was no significant difference between the control and the treated rats in their body weight measured always on the same day of the week (Monday) (Supplementary Figure 3A). Estimated marginal means of the weekly body weights were significantly dependent on the rats' age (Supplementary Figure 3B) showing a significant decrease with increasing age, but the treatment had no effect on the weight gain, and there was no interaction between the treatment weeks (that is, age of the rats) and treatment doses. In groups LD and MD, the rate of weight gain was lower than in groups VT and HD (Supplementary Figure 3C).

From the organs examined, the body weight related weight of the lungs, kidneys, brain, and liver is shown in Supplementary Table 1. Lung, kidney, and liver weights were affected but not the brain weight. Other organs, ie, spleen and heart, were not affected either.

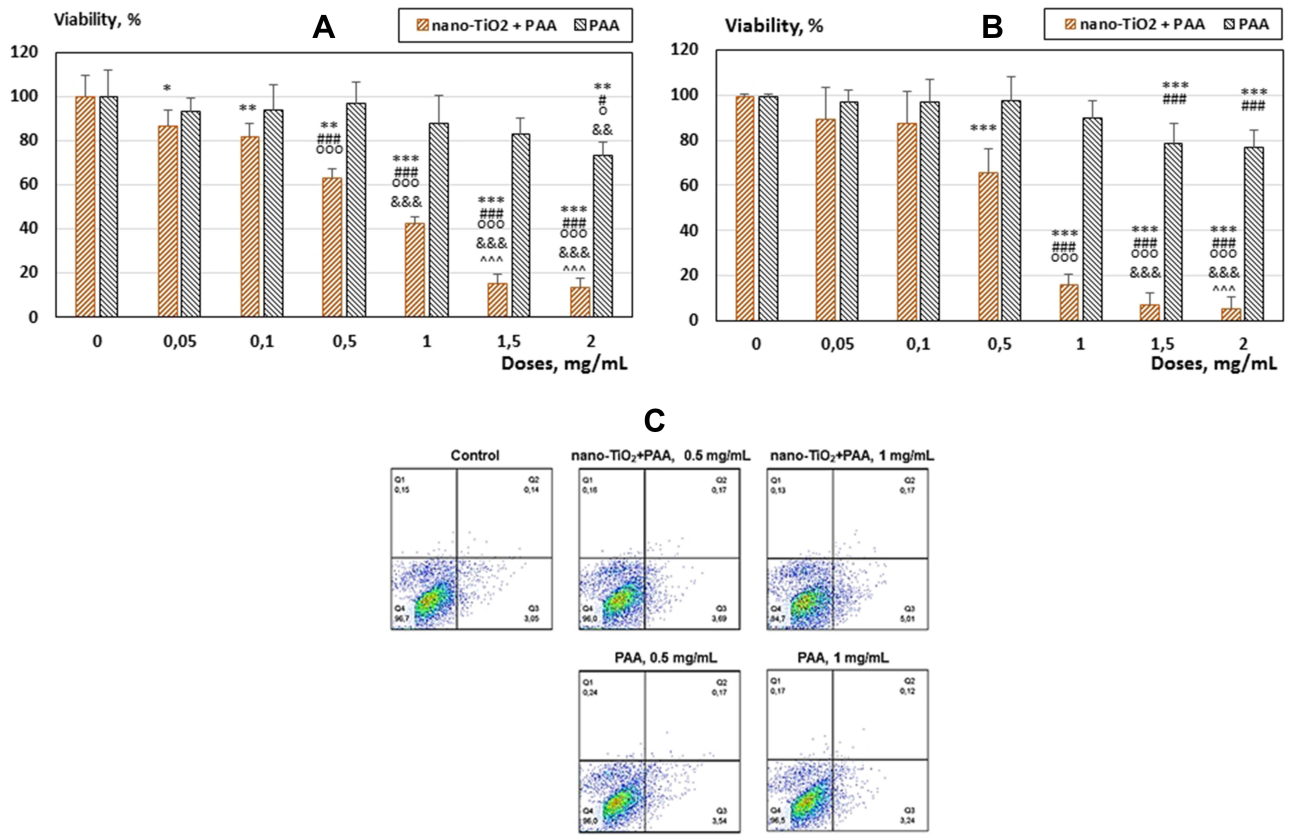

Figure 2 The effect of nano-TiO_2 treatment on the survival of the cultured astrocytes. Dose-dependent decrease of viability after 24 hours (**A**) and 48 hours (**B**) of exposure to TiO_2 nanorods or the vehicle (PAA). (**C**) flow cytometry graphs showing no difference in apoptosis (quadrants Q2 and Q3) and necrosis (quadrant Q1) between control and treated cells.

Notes: Bar graphs: means+SD, n=4. *, **, ***; p<0.05, 0.01, 0.001 vs 0 mg/mL dose; #, ### p<0.05, 0.001 vs 0.05 mg/mL dose; °°°p<0.001 vs 0.1 mg/mL dose; &&&p<0.001 vs 0.5 mg/mL dose; ^^^p<0.001 vs 1 mg/mL dose.

Abbreviations: PAA, polyacrylic acid; SD, standard deviation; TiO_2, titanium oxide.

Biochemical and Pathomorphological Changes in the Treated Rats' Lungs and Kidneys

Increased oxidative stress in the lungs was indicated both by a non-enzymatic (lipid peroxidation) and an enzymatic (catalase activity) parameter as shown in Supplementary Figure 4. In the lungs of rats treated identically in a previous study, several pro-inflammatory cytokines (such as IL-1α and CINC1) were elevated, and these findings are in line with the changes of the oxidative stress indicators presented in this study.[16]

Light microscopy of HE stained lung sections showed histological alterations in the nano-TiO_2 treated rats. Intermingled areas with mild atelectasis or emphysema were seen with destroyed alveolar septa in the latter. In the atelectatic areas, blackish–brown pigmented particles were found in the cytoplasm of macrophages or extracellularly, the latter surrounded by focal minimal lymphocytosis, hyperemia, and non-specific extravasation, as also seen previously.[16]

In contrast, the structure of the kidney cortex and medulla was not altered in any of the treated groups. No inflammatory reaction or focal extravasation was induced by the nanorods. Moreover, no macrophages (histiocytes) with phagocyted NPs were observed in the kidney sections by light microscopy (not shown).

However, the TEM images of lung tissue samples from control and treated rats (Figure 3) showed sharp-contoured, elongated objects, which were supposed (and subsequently confirmed, see Figure 4) to be TiO_2 nanorods only in the treated rats' lungs (groups LD, MD, and HD). In these groups, phagolysosomes laden with these dense nanorods were seen in interstitially localized macrophages. In group HD, the phagolysosomes seemed to have a damaged membrane, suggesting disturbed lysosomal flux as a source of cell damage. Nanorods were observed also free in the cytoplasm and near to or attached to organelles (mitochondria or endoplasmic reticulum). In the controls (C and VT), the small, round, blurred grains were

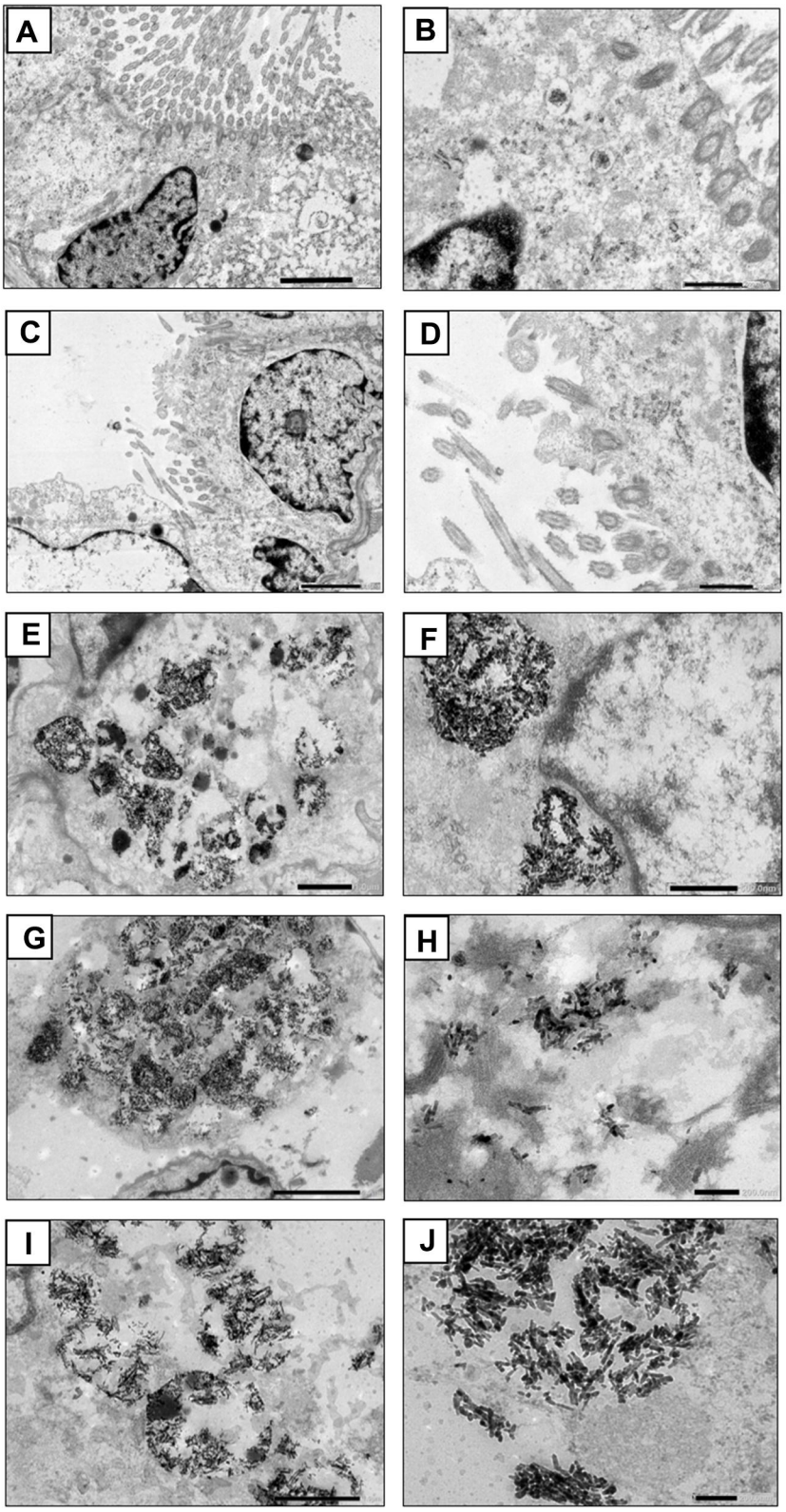

Figure 3 Transmission electron micrographs of lung sections from group C ((**A**) 5000×, scale bar 2 μm; (**B**) 15,000×, scale bar 500 nm); VT ((**C**) 4000×, scale bar 2 μm; (**D**) 12,000×, scale bar 500 nm); LD ((**E**) 5000×, scale bar 1 μm; (**F**) 12,000×, scale bar 500 nm); MD ((**G**) 4000×, scale bar 2 μm; (**H**) 12,000×, scale bar 200 nm); and HD ((**I**) 8000×, scale bar 1 μm; (**J**) 20,000×, scale bar 200 nm).

Abbreviations: C, control; VT, vehicle treated; LD, low dose treated; MD, medium dose treated; HD, high dose treated.

dissimilar to the above mentioned elongated objects (these grains contained Pb, Si, and U, and might be impurities caused by the histological work).

By applying higher magnification and EDS analysis, the identity of the elongated objects could be confirmed. Figure 4 shows clusters of dense nanorods, probably from disintegrated multivesicular bodies near the nuclear membrane of an alveolar macrophage (TEM image, Figure 4A). The presence of Ti was verified by EDS applied on the clusters; the spectrum in Figure 4C was taken from the

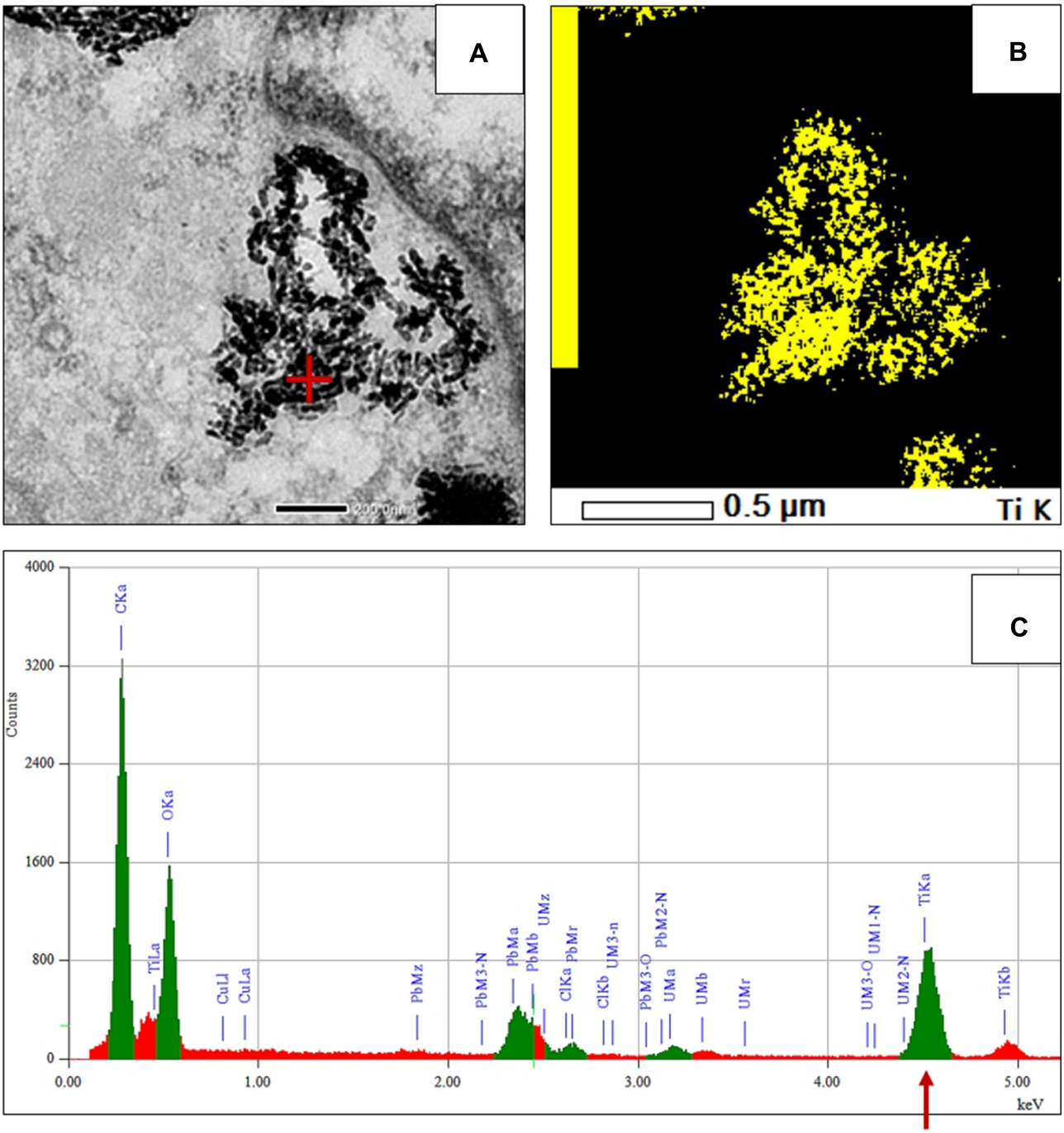

Figure 4 The presence of TiO_2 nanorods in the lung tissue of a treated rat from the high dose (HD) group. (**A**) Transmission electron micrograph (80,000×, scale bar 200 nm) of nanorods clumped in a roundish object, probably a disintegrated multivesicular body. (**B**) Energy dispersive spectroscopic mapping shows presence of Ti in the nanorods visualized in A. (**C**) spectrum taken from the area marked by red cross in (**A**) featuring a very strong TiO_2 Kα peak (arrow).
Abbreviations: Ti, titanium; TiO_2, titanium oxide.

spot marked by the red cross in the biggest cluster. The identical shape of the nanorod clusters in Figure 4A and the Ti-positive sites on the EDS map in Figure 4B proved that the dense elongated objects were in fact Ti-containing NPs.

In the kidney cortex of treated rats, the dense objects were seen in the glomeruli and in proximal tubular epithelial cells free in the cytoplasm or attached to organelles, especially to mitochondria, and engulfed in lysosomes like in the lung tissue. Figure 5 shows that similarly to what was observed in the lungs, small, roundish granules were seen in the control rats' samples, in the cytoplasm and mitochondria of tubular epithelial cells (group C, Figure 5A and B) or in smooth muscle cells (group VT, Figure 5C and D). Rod-shaped objects appeared only in treated animals' renal tissue; in the mesenchyme (group LD, Figure 5E and F), in distal tubular epithelial cells, free or associated to lysosomes (group MD, Figure 5G and H), or the cytoplasm of an endothelial cell (group HD, Figure 5I and J). In the renal medulla of HD rats, however, no nanorods, only small, unsharply contoured, roundish granules (like those in the control rats) were observed (Figure 5K and L). Figure 6 shows the result of the EDS analysis on kidney sections. NPs around and adhered to a mitochondrion in a cortical tubular epithelial cell of a rat from group MD are seen in Figure 6A. Again, the overlap of the visualized particles with the Ti-positive spots in Figure 6B verified that TiO_2 nanorods were present in the kidneys.

Ruptured phagolysosomes, nanorods attached to mitochondria and near the nuclear membrane, together with the detected oxidative stress in case of the lungs, suggested cell damage. The TEM images of lung and kidney tissues, however, showed no clear signs of apoptosis. Hence, apoptosis detection was applied on the lung and kidney samples by means of TUNEL assay. As seen in Figures 7 and 8, there was a dose-dependent increase of TUNEL positive (that is, apoptotic) cells in the same treated rat's lung (alveolar region) and kidney cortex samples (glomerulus and the surrounding tubules), respectively, and the change in the groups MD and HD was significant.

The presence of TiO_2 nanorods and cell loss was thus verified in the treated rats' lungs and kidneys and also in cultured astrocytes. This, and the (albeit moderate) increase in brain Ti content in the treated rats suggested that the nervous system may also be affected.

Changes in the Cortical and Peripheral Electrophysiological Nervous Activity

The general trend of change in the evoked forms of cortical electrical activity in the treated rats was slowing. Latency lengthening of the cortical EPs was present in all three modalities (Figure 9). The extra lengthening of latency of SS EPs with increasing stimulation frequency was also more pronounced in the treated rats (Figure 9A). The amplitude was also measured on the SS EPs, and the frequency-dependent decrease of mean amplitude of the 50 EPs in a series was dose-dependently stronger in the treated rats compared to mean EP amplitude of the controls (Figure 9B). The latter change implied increased fatigue (a possible sign of insufficient energy supply) of the ascending somatosensory pathway, which was also observed on the ratio of the latency of the last and first SS EPs within the series of 50 (Figure 9C). The VIS and AUD EPs also showed significant dose-dependent latency lengthening (Figure 9D).

The frequency spectrum of the spontaneous cortical activity was characterized by the ECoG index (see Methods). Its decreasing trend, indicating relatively more high frequency and/or less low frequency components, was uniform for all three cortical areas but remained below significance (Supplementary Figure 5).

The response, obtained in the CPu by stimulating the motor cortex characterizing cortico-subcortical motor control, was also affected. Both peaks of the biphasic response had increased latency in the HD group, and the first peak also in the MD group (Figure 10).

CAP of the tail nerve, obtained from control and treated rats, indicated decreased conduction velocity and increased relative refractory period vs controls (Figure 11A). Both effects were dose-dependent. In the treated rats, the decrease of conduction velocity with increasing stimulation frequency was also more intense (Figure 11B). This and the data of the refractory period showed that the tail nerve in TiO_2-exposed rats was less able to follow frequent stimulation (an effect that was in line with the frequency-dependent latency increase of the SS Eps, shown in Figure 9).

The dose-dependence of changes in the electrophysiological parameters and tissue Ti levels suggested a causal relationship, which was further examined by obtaining the correlation of SS EP latency and cortical Ti levels as well as tail nerve conduction velocity and blood Ti levels. The

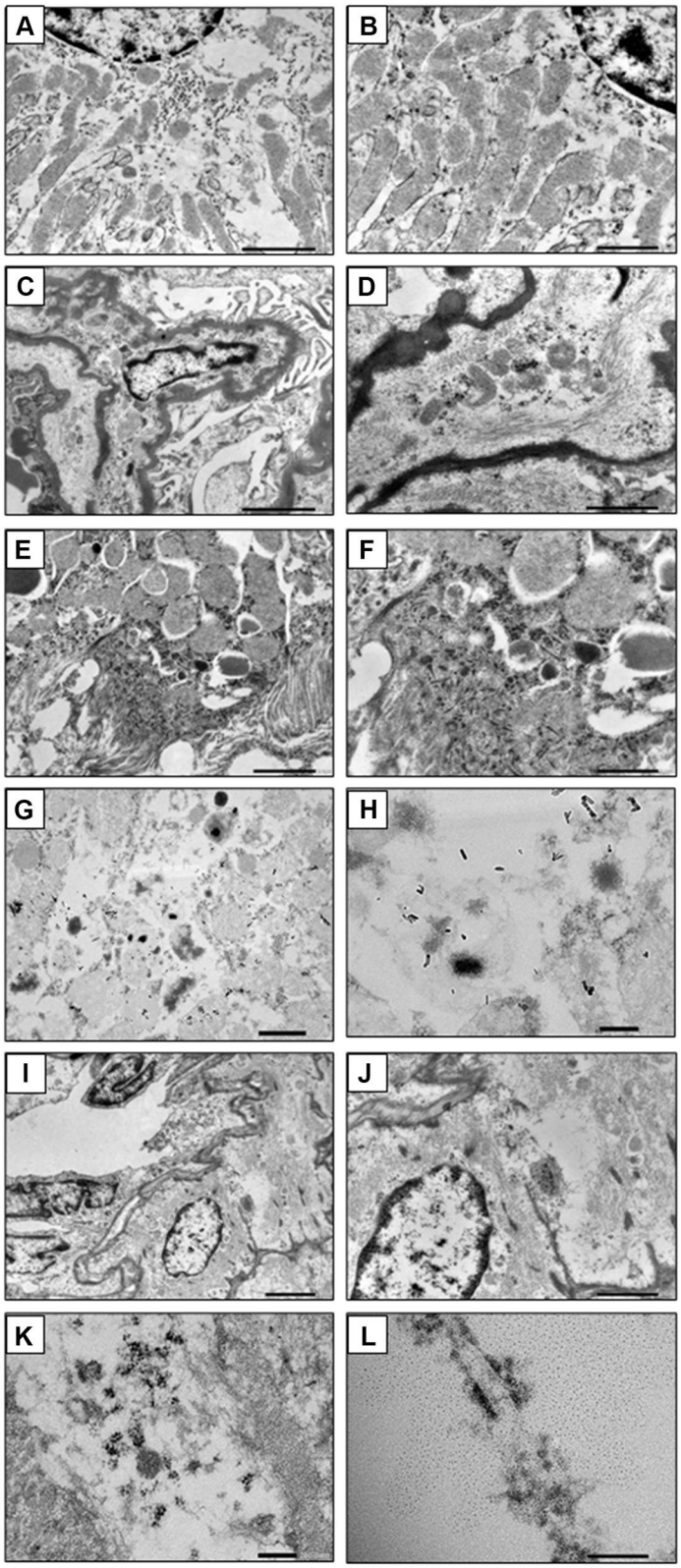

Figure 5 (**A**–**J**) Transmission electron micrograms of kidney cortical sections from group C ((**A**) 6000×, scale bar 2 μm; (**B**) 10,000×, scale bar 1 μm); VT ((**C**) 6000×, scale bar 2 μm; (**D**) 12,000×, scale bar 1 μm); LD ((**E**) 5000×, scale bar 2 μm; (**F**) 10,000×, scale bar 1 μm); MD ((**G**) 5000×, scale bar 1 μm; (**H**) 20,000×, scale bar 200 nm); HD ((**I**) 4000×, scale bar 2 μm; (**J**) 10,000×, scale bar 1 μm). (**K** and **L**) Kidney medullar sections from group HD ((**K**) 20 000×, scale bar 200 nm; (**L**) 60,000×, scale bar 100 nm).
Abbreviations: C, control; VT, vehicle treated; LD, low dose treated; MD, medium dose treated; HD, high dose treated.

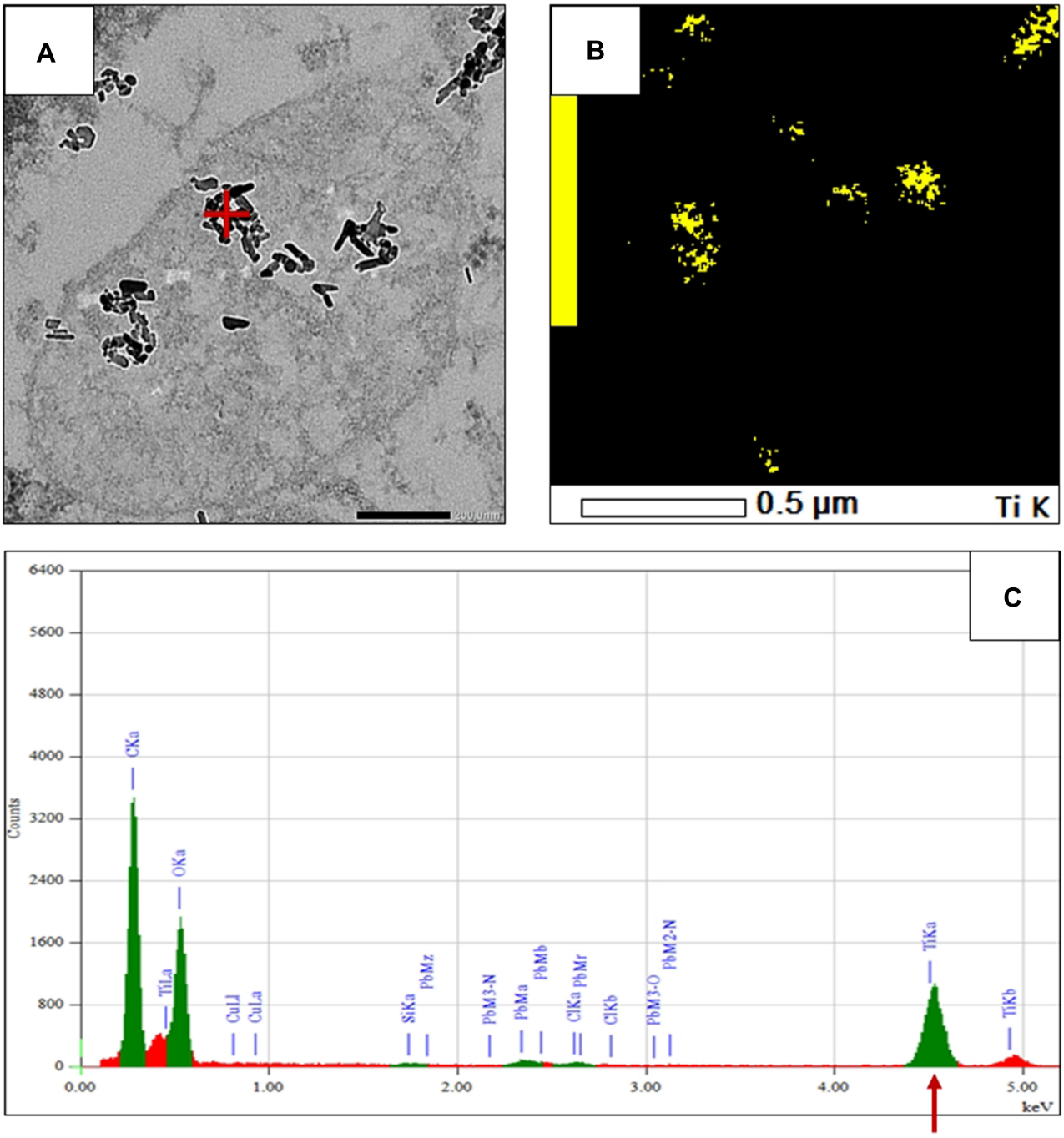

Figure 6 Presence of TiO_2 nanorods in the kidney cortical tissue of a treated rat from the medium dose (MD) group. (**A**) Transmission electron micrograph showing nanorods attached to a mitochondrion (25,000×, scale bar 200 nm). (**B**) Energy dispersive spectroscopic mapping shows presence of Ti in the nanorods visualized in (**A**). (**C**) spectrum taken from the area marked by red cross in (**A**) featuring a very strong TiO_2 Kα peak (arrow).
Abbreviations: Ti, titanium; TiO_2, titanium oxide.

correlations were fair (Supplementary Figure 6) as measured in cortical and peripheral electrophysiological changes providing and indirect proof that all detected neuro-functional effects had the same background, presence of elevated amounts of Ti, in form of NPs, and the NPs' cellular effects.

Discussion

In this work, intratracheal application of TiO_2 nanorods resulted in elevated Ti levels in tissue samples of the lungs, brain, and kidneys, as well as in blood; moreover, in lung and kidney samples, the presence of nanorods was directly confirmed. This meant that the treatment resulted

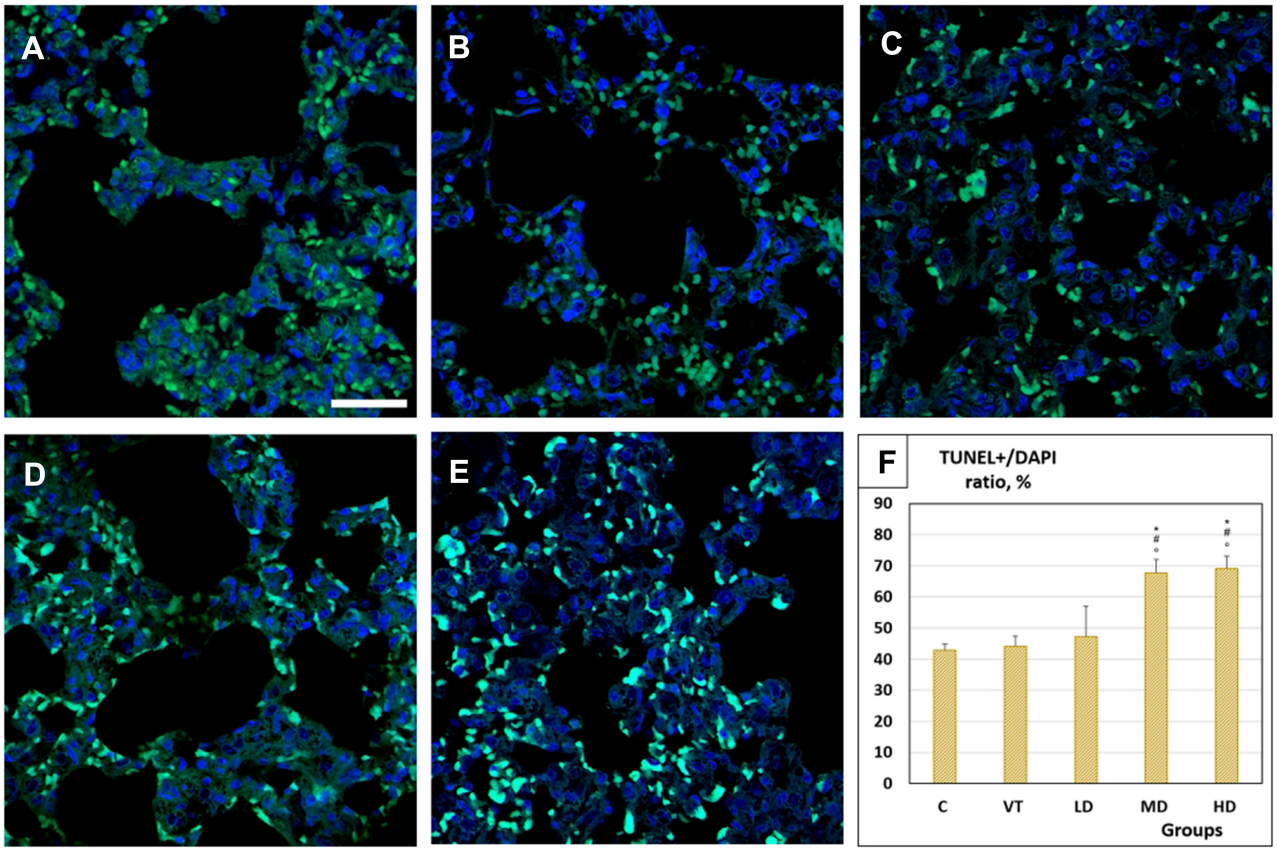

Figure 7 Apoptosis detection in lung tissue sections. Sample micrographs: (**A**) group C; (**B**) group VT; (**C**) LD; (**D**) MD; (**E**) HD. Scale bar 50 μm. Bar graph, (**F**) Ratio of TUNEL positivity and DAPI staining showing significantly elevated number of apoptotic cells in sections from MD and HD rats.
Notes: Green, TUNEL staining; blue, DAPI staining. Bar graph: Means+SD, n=3 or 6 (see Methods); *p<0.05 vs C; #p<0.05 vs VT; °p<0.05 vs LD.
Abbreviations: TUNEL, terminal deoxynucleotidyl transferase dUTP nick end labeling; DAPI, 4′,6-diamidino-2-phenylindole; C, control; VT, vehicle treated; LD, low dose treated; MD, medium dose treated; HD, high dose treated.

in an effective internal dose, which was probably responsible for the tissue/cell damages and neuro-functional alterations observed. In parallel to that, TiO_2 nanorods were detected attached to treated cultured astrocytes in vitro. The in vivo doses applied here were in the same range as it has been found effective in previous works with spherical TiO_2 NPs.[30,49] Compared to the human exposure limit mostly referred to (0.3 mg/m^3 for nano-TiO_2; NIOSH),[51] our in vivo doses were about two orders of magnitude higher, but the time span of application (28 times over 6 weeks) was rather short. Details of this comparison were described in Ref. 16.

The highest Ti level was measured in the lung samples, suggesting deposition of a considerable fraction of the applied nanorods in that organ. It was partly in line with a paper reporting that TiO_2 NPs instilled to rats were completely retained in the lungs for several days.[52] However, in our case, detectable amounts of the administered NPs passed the alveolar barrier, in which macrophages may have played a role by migrating from the alveolar space to the interstitium after engulfing, but not decomposing the amounts of NPs (see NP-laden phagolysosomes in Figure 3).

In the lungs themselves, the subacute exposure to TiO_2 nanorods resulted in tissue damage, which manifested in mild atelectasis or emphysema, and macrophages with phagocyted NPs were observed by TEM. Beyond such pathomorphological changes, increased apoptosis (TUNEL positivity, see Figure 7) indicated the damage caused by the TiO_2 nanorods in the treated rats' lungs. After a single intratracheal instillation of 25 nm spherical TiO_2 NPs, dose-dependent occurrence of neutrophil infiltration and granulomatous lesions were described in the rat lungs.[53] When mice were instilled with very small (<10 nm) anatase TiO_2 NPs for 90 days, dose-dependently increased relative lung weight, increased oxidative stress markers, and various histopathological alterations including emphysema were found,[54] similarly to our in vivo observations in rats.

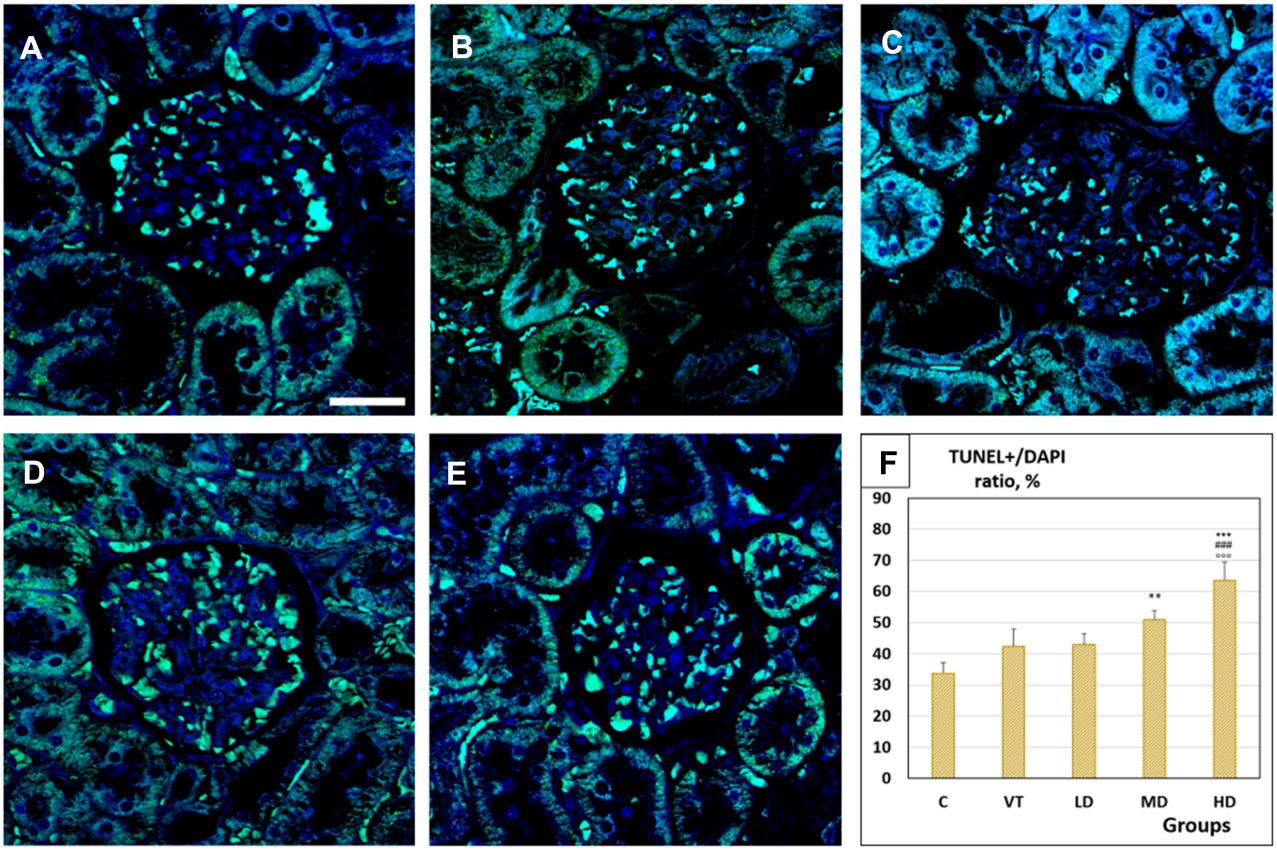

Figure 8 Apoptosis detection in kidney cortical tissue sections. Sample micrographs: (**A**) group C; (**B**) group VT; (**C**) group LD; (**D**) group MD; (**E**) group HD. Scale bar 50 μm. Bar graph, (**F**) Ratio of TUNEL positivity and DAPI staining showing significantly elevated number of apoptotic cells in sections from MD and HD rats.
Notes: Greenish–blue, TUNEL staining; blue, DAPI staining. Bar graph: Means+SD, n=3 or 6 (see Methods). **, ***p<0.01, 0.001 vs C; ###p<0.001 vs VT; °°°p<0.001 vs LD.
Abbreviations: TUNEL, terminal deoxynucleotidyl transferase dUTP nick end labeling; DAPI, 4′,6-diamidino-2-phenylindole; C, control; VT, vehicle treated; LD, low dose treated; MD, medium dose treated; HD, high dose treated.

Human lung damage (functional loss, elevated markers of oxidative stress, and inflammation) on exposure to airborne nano-TiO_2 has also been reported.[13]

The results of chemical Ti measurement (Supplementary Figure 2), and partly of TEM-EDS identification of the NPs (Figures 4 and 6), showed that the instilled nanorods could pass the lungs (traveling probably in macrophages as mentioned above) and reach the blood and distant organs, notably the kidneys and the brain. Similarly to the lungs (site of entry for the TiO_2 NPs), nanorods were identified (Figure 6) and apoptotic cell damage detected by TUNEL assay (Figure 8) in the cortex of kidneys (the organ where NPs are accumulated and/or excreted). Because of technical difficulties, EDS has infrequently been applied to tissue specimens, but in this case, successful application was crucial in the identification of TiO_2 NPs. In rats orally treated with 10 nm anatase NPs (100 mg/kg BW, 2 months), the kidneys showed Ti accumulation, functional damage, and abnormal glomerular morphology with the infiltration of mononuclear cells, and these effects were counteracted by an antioxidant.[55]

The cited data and our results suggest that apoptosis may be one of the final outcomes of cell damage induced by nanoparticulate TiO_2 in different tissues and organs and that this cell damage is largely due to oxidative stress. In vitro, cell lines of human lung origin showed increased ROS generation and apoptotic death on exposure to spherical TiO_2 NPs (of <50 nm size and anatase crystal structure).[56] Mitochondrial damage (depolarization), lipid peroxidation, and other features of oxidative stress were also described in cell lines of glial origin, treated with anatase NPs of <50 nm size,[57] which is in line with viability loss seen in our work on mouse astrocytes exposed to TiO_2 nanorods (Figure 2).

Generally, tissues of high energy demand and rich in mitochondria may be especially vulnerable to damage by NPs; the NPs' migration to mitochondria and the impeding oxidative phosphorylation may be involved in that.[22]

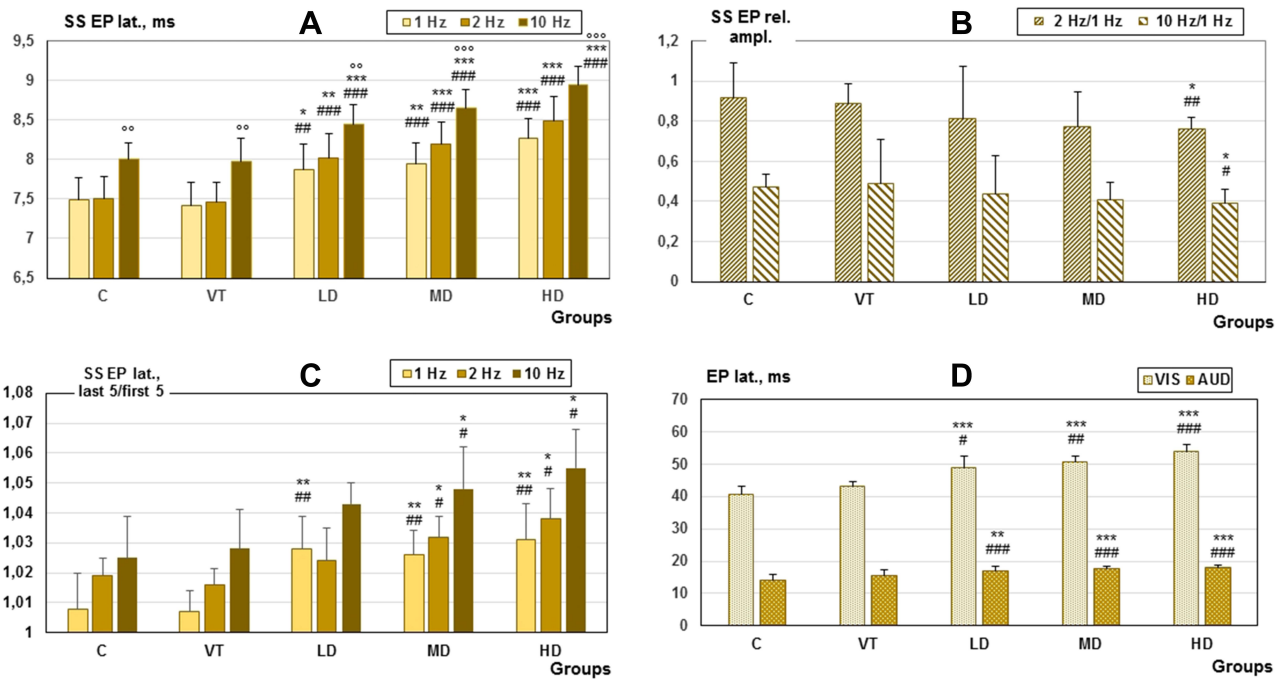

Figure 9 Effect of TiO_2 nanorods on the cortical evoked potentials. (**A**) Latency of the SS EP in control and treated rats at 1, 2 and 10 Hz stimulation frequency. (**B**) Fatigue in the SS EPs, demonstrated by relative amplitudes. (**C**) Fatigue in the SS EPs demonstrated by the ratio of the latency of the last and first EPs. (**D**) Latency of the VIS and AUD EPs in control and treated rats.

Notes: Means+SD, n=10. *, **, ***p<0.05, 0.01, 0.001 vs C; #, ##, ###p<0.05, 0.01, 0.001 vs VT; °°, °°°p<0.01, 0.001 vs 1 Hz stimulation within the same treatment group.

Abbreviations: C, control; VT, vehicle treated; LD, low dose treated; MD, medium dose treated; HD, high dose treated; EP, evoked potential; SS, somatosensory; VIS, visual; AUD, auditory; TiO_2, titanium oxide.

In the present work, nanorods were identified around the mitochondria and attached to them in 10^5x magnification TEM images from the kidney cortex of the MD rats. Similar to the observed glomerular capillary endothelial and proximal tubular epithelial cells, organelle-specific deposition of TiO_2 NPs and disturbed cell signaling related to mitochondrial dysfunction[58] may also be present in other mitochondria-rich tissues, such as skeletal and heart muscles, or in certain parts of the nervous system.[59,60]

When neuronal and glial cell lines of human origin were exposed in vitro to 15 nm TiO_2 NPs, damage to the mitochondria (together with ROS generation) was found.[33] On treating primary astrocytes isolated from rat pups with variations of nano-TiO_2, including 50 nm spherical anatase at concentrations similar to those in our in vitro experiment, substantial viability loss, elevated ROS production, mitochondrial deterioration, and impaired glutamate uptake were observed.[61] In mitochondria isolated from rat brain, indicators of oxidative damage were increased and reactions of terminal oxidation were decreased on treatment with 30 nm nano-TiO_2, highlighting the role of mitochondrial damage in the neurotoxicity of TiO_2 NPs.[62]

Kidney and liver are also organs of high energy turnover. Intravenously applied nano-TiO_2 (10–20 nm, spherical) caused massive oxidative stress, DNA damage, and mitochondria-mediated apoptosis in the kidneys and liver of rats.[63] The changes of relative weight and Ti content of these organs were similar to those observed in the present study (Supplementary Table 1, Supplementary Figure 2). With oral application of nano-TiO_2 to rats, apoptosis in the proximal tubules, together with histological and functional damage, and attenuation of the damages by the antioxidant quercetin, has been described.[17]

To reach the brain, TiO_2 NPs must cross the BBB or migrate along afferent nerve fibers; both of these mechanisms have been described as feasible.[18] In contrast, the access of free Ti ions to the brain, released from the surface of the NPs in the low pH interior of phagosomes, is not likely because of the minimal solubility of TiO_2 NPs.[64] Consequently, the chemical detection of Ti in brain and other tissues was a sufficient proof of presence of TiO_2 NPs in our work. Rats inhaling nano-TiO_2 have been

reported to show damage in BBB, which may promote the uptake of the nanorods into the brain.[25]

TiO_2 nanorods, reaching the brain substance, could induce the functional alterations described above by inducing oxidative stress and/or neuroinflammation, and finally apoptosis.[65] If membrane lipids are oxidized, membrane fluidity can change affecting axonal conduction and synaptic transmission, both of which depend on the normal functioning of the cell membrane.[65] In a previous study with spherical TiO_2 NPs, TBARS reaction (used to indicate oxidative stress in the present study as well) was increased in the brain and lung samples of rats receiving 10 mg/kg BW nano-TiO_2 for 28 days; and the latency increase of SS EP (regarded in the present work as the indicator of functional damage) was proportional to the level of both Ti and TBARS in the brain.[30] In a study with another metal oxide NP (MnO_2), treatment with an antioxidant reversed the alterations of cortical electrical activity, similarly to those seen in the treated rats in the present work, which argued for the role of oxidative mechanism in NP-induced neuro-functional damage.[66]

Numerical parameters (eg, latency and amplitude) of sensory cortical EPs reflect changes both in axonal conduction and synaptic transmission. Both processes depend highly on mitochondrial energy production, and so these parameters may serve as sensitive biomarkers of neurotoxicity. Energy shortage resulting from NP-induced mitochondrial damage affects neuronal and glial cells alike. Among glial cells, astrocytes fulfil the function of supporting neuronal activity in various ways. These cells remove glutamate, the most important excitatory transmitter in the CNS, from the synaptic cleft by a co-transport with Na^+ along the concentration gradient of the latter, metabolize it to glutamine, and supply that as a transmitter precursor for both glutamatergic and GABAergic neurons.[67] The decrease in transmitter turnover supported by the astrocytes, due to cell/function loss reported in[60] and observed in our in vitro model, may disturb the balance of excitation and inhibition, partly due to excess free glutamate, and partly to loss of negative feedback between glutamate and GABA, in case glutamate-uptake induced GABA release from the astrocytes is missing.[68] Finally, failing glutamate transport, due to NP-induced astrocyte damage manifested in reduced ion pump or enzyme activity, may result in an abnormally high perisynaptic glutamate level, which will disturb transmission.[69]

Ion pumps weakened by energy shortage also affect transmembrane ion gradients involved in nerve pulse conduction. A similar pattern of changes in EP latency and tail nerve conduction velocity suggested that the effect of TiO_2 nanorods on axonal conduction and synaptic transmission was both involved in the mechanism of the observed changes. Increased fatigability of the SS sensory pathway (Figure 9B and C) and the tail nerve (Figure 11) in the treated rats might also point to energy shortage.

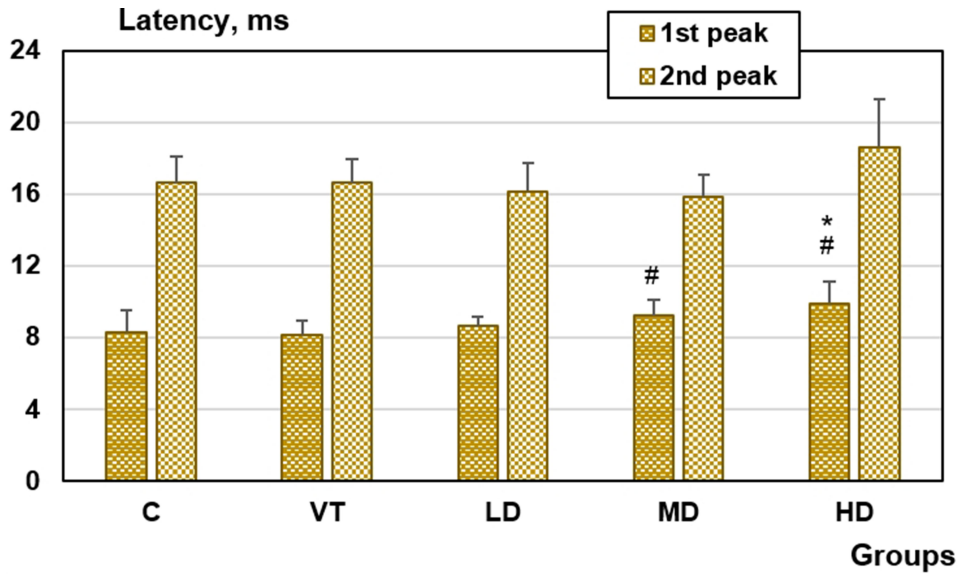

Figure 10 Latency of the biphasic evoked response recorded from the CPu on stimulating the motor cortex in the control and treated rats.
Notes: Means+SD, n=10. *p<0.05 vs C; #p<0.05 vs VT.
Abbreviations: C, control; VT, vehicle treated; LD, low dose treated; MD, medium dose treated; HD, high dose treated; CPu, caudato-putamen.

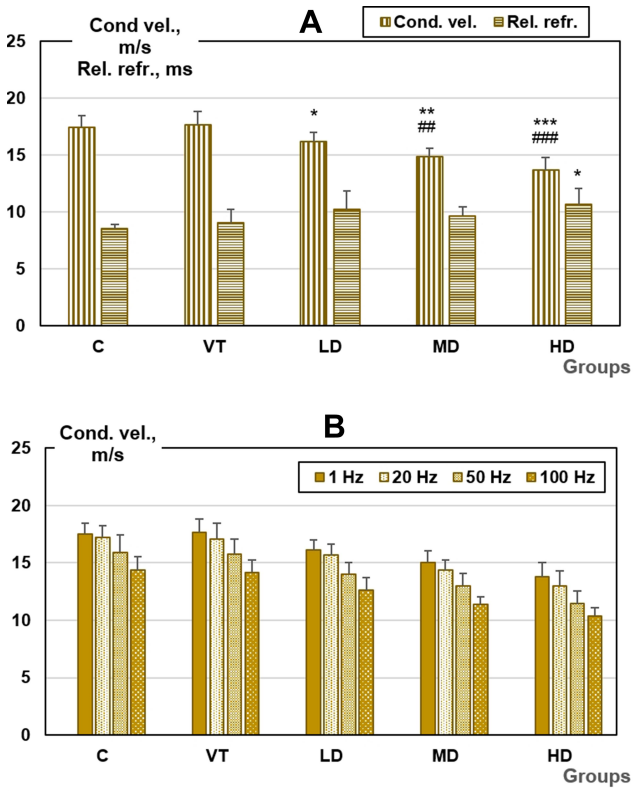

Figure 11 Conduction velocity and relative refractory period of the rats' tail nerve (**A**) and frequency dependence of the conduction velocity (**B**).
Notes: Means+SD, n=10. *, **, ***p<0.05, 0.01, 0.001 vs C; ##, #### p<0.01, 0.001 vs VT.
Abbreviations: Cond. vel., nerve conduction velocity; Rel. refr., relative refractory period; C, control; VT, vehicle treated; LD, low dose treated; MD, medium dose treated; HD, high dose treated.

Slowed corticostriatal evoked response (Figure 10) might indicate altered motor control in the treated rats. Caudatoputamen, the site of recording, is a key element in striatal plasticity, and thus in adaptive motor control and procedural memory.[70] In our previous studies, altered open field and grip strength test performance were detected in rats treated with spherical TiO_2 NPs.[49,71] In mice, deterioration of spatial memory, together with biochemical and electrophysiological signs of neuronal damage, have been reported.[18]

In a state of energy shortage due to mitochondrial damage, spontaneous cortical activity is expected to become slower as it is known in mitochondriopathies.[72] The mild shift of ECoG to higher frequencies (see Supplementary Figure 5) observed in the present work is in contrast to that, but fits well, together with lengthened EP latencies, with decreased cholinesterase activity, an effect described in rats after a 2-month oral treatment with TiO_2 NPs.[26] If the ascending reticular cholinergic activation of the cortex is abnormally strong, spontaneous cortical activity will be increased, leading to depressed evoked activity.[73,74]

It was found in the present work that anatase TiO_2 nanorods, applied to the airways of rats by intratracheal instillation, reached the blood and various organs including the kidneys, the liver, and the CNS. Locally detected Ti levels and relative weights of the investigated organs, apoptotic cell death in the lungs and kidneys, and alterations in central and peripheral electrophysiological nervous activity were mostly proportional to the applied doses and reached a significant level in animals receiving the high or high and medium dose. Viability loss of cultured astrocytes, used as an in vitro model of CNS effect, was also dose-dependent. This suggested a causal relationship of treatments and effects. Based on the localization of the visualized nanorods and on literature data, mitochondrial damage, oxidative stress, and apoptotic cell death were likely involved in the toxic mechanism.

The mentioned widespread application of rod-shaped and other TiO_2 NPs makes human exposure likely, which in turn may contribute to the causation or aggravation of several chronic non-infectious diseases of the organs investigated in the present study (asthma COPD, chronic renal insufficiency, as well as neurological diseases, eg, Leigh's syndrome of MERRF). Persons having such diseases may be at increased risk in case of job-related exposure to TiO_2 NPs. Oxidative stress, possibly caused by NPs, is probably involved in the mechanism of hypertension, a widespread chronic disease in itself and risk factor of further circulatory and central nervous diseases.[75] Inhaled TiO_2 nanorods and other metal-containing NPs were found to be associated with mitochondrial damage, protein misfolding, and other subcellular abnormalities leading to neurodegenerative disorders early in life.[76]

The effects observed in the present work were mostly in line with the effects described in studies with other shapes and/or sizes of nano-TiO_2. This and the probable health consequences in humans underline the importance of gaining comprehensive toxicological information on TiO_2 nanorods, a nanomaterial with widespread application.

Conclusion

In the present work, subacute intratracheal exposure of rats to anatase TiO_2 nanorods resulted in pathomorphological alterations in the lungs and kidneys and functional alterations in the CNS, with directly or indirectly verified presence of the nanorods in the affected organs. However, no clinical signs of toxicity were observed. The damages were likely due to apoptotic cell death initiated by NPs

affecting, first of all, the mitochondria and causing oxidative stress.

The lungs, kidneys, and the CNS are involved in several chronic diseases of humans, in the background of which oxidative stress and chronic inflammation were identified or supposed. It is possible that exposure to nano-TiO_2, whether related to jobs, environmental pollution, or certain consumers' goods, may contribute to their causation or aggravation. On the one hand, this is one more reason why adequate safety measures, based on research data, are needed. On the other hand, the results of the present work may provide the base of developing effect biomarkers of TiO_2 and other NPs for human application.

Acknowledgments

The authors are thankful to Dr Gábor Galbács and colleagues, Department of Inorganic and Analytical Chemistry, Faculty of Science and Informatics, University of Szeged, Hungary for the ICP-MS measurements.

Financial support by the National Research, Development and Innovation Office-NKFIH through projects GINOP-2.3.2-15-2016-00038 and EFOP-3.6.1-16-2016-00008 is gratefully acknowledged. Furthermore, this work was supported by the grants UNKP-19-4-SZTE-14 and UNKP-20-5-SZTE-655 of the New National Excellence Program of the Ministry for Innovation and Technology (M.K.) and by the János Bolyai Research Scholarship of the Hungarian Academy of Sciences (BO/00878/19/8 for M.K.).

Tamara Horváth's present address is Department of Experimental Surgery, Faculty of Medicine, University of Szeged, Szeged.

Disclosure

The authors report no conflicts of interest in this work.

This work is partially based on the PhD thesis of Tamara Horváth (Szeged, 2019).

References

1. Musial J, Krakowiak R, Mlynarczyk DT, Goslinski T, Stanisz BJ. Titanium dioxide nanoparticles in food and personal care products – what do we know about their safety? *Nanomaterials*. 2020;10:1110. doi:10.3390/nano10061110
2. Chen J, Poon C. Photocatalytic construction and building materials: from fundamentals to applications. *Build Environ*. 2009;44(9):1899–1906. doi:10.1016/j.buildenv.2009.01.002
3. Chatha SAS, Asgher M, Asgher R, et al. Environmentally responsive and anti-bugs textile finishes – recent trends, challenges, and future perspectives. *Sci Total Environ*. 2019;690:667–682. doi:10.1016/j.scitotenv.2019.06.520
4. Dastjerdi R, Montazer M. A review on the application of inorganic nano-structured materials in the modification of textiles: focus on anti-microbial properties. *Colloids Surf B Biointerfaces*. 2010;79(1):5–18. doi:10.1016/j.colsurfb.2010.03.029
5. Buzea C, Pacheco II, Robbie K. Nanomaterials and nanoparticles: sources and toxicity. *Biointerphases*. 2007;2(4):MR17–MR172. doi:10.1116/1.2815690
6. Nel A, Yia T, Mädler L, Li N. Toxic potential of materials at the nanolevel. *Science*. 2006;311(5761):622–627. doi:10.1126/science.1114397
7. Zhou D, Han S, Yan T, et al. Toxicity of titanium dioxide nanoparticles induced by reactive oxygen species. *Reactive Oxygen Species*. 2019;8(23):267–275.
8. Guerra-Araiza C, Álvarez-Mejía AL, Sánchez-Torres S, et al. Effect of natural exogenous antioxidants on aging and on neurodegenerative diseases. *Free Rad Res*. 2013;47(6–7):451–462. doi:10.3109/10715762.2013.795649
9. Gyurászová M, Gurecká R, Bábíčková J, Tóthová L. Oxidative stress in the pathophysiology of kidney disease: implications for noninvasive monitoring and identification of biomarkers. *Oxidative Med Cell Longevity*. 2020;5478708.
10. Czajka M, Sawicki K, Sikorska K, et al. Toxicity of titanium dioxide nanoparticles in central nervous system. *Toxicol in Vitro*. 2015;29(5):1042–1052. doi:10.1016/j.tiv.2015.04.004
11. Gui S, Zhang Z, Zheng L. Molecular mechanism of kidney injury of mice caused by exposure to titanium dioxide nanoparticles. *J Hazard Mater*. 2011;195:365–370. doi:10.1016/j.jhazmat.2011.08.055
12. Grande F, Tucci P. Titanium dioxide nanoparticles: a risk for human health? *Mini Rev Med Chem*. 2016;16(9):762–769. doi:10.2174/1389557516666160321114341
13. Zhao L, Zhu Y, Chen Z, et al. Cardiopulmonary effects induced by occupational exposure to titanium dioxide nanoparticles. *Nanotoxicology*. 2018;12(2):169–184. doi:10.1080/17435390.2018.1425502
14. Noël A, Charbonneau M, Cloutier Y, Tardif R, Truchon G. Rat pulmonary responses to inhaled nano-TiO2: effect of primary particle size and agglomeration state. *Part Fibre Toxicol*. 2013;10:48. doi:10.1186/1743-8977-10-48
15. Horváth T, Papp A, Igaz N, et al. Pulmonary impact of titanium dioxide nanorods: examination of nanorod-exposed rat lungs and human alveolar cells. *Int J Nanomed*. 2018;13:7061–7077. doi:10.2147/IJN.S179159
16. Fadda LM, Mohamed AM, Ali HM, Hagar H, Aldossari M. Prophylactic administration of carnosine and melatonin abates the incidence of renal toxicity induced by an over dose of titanium dioxide nanoparticles. *J Biochem Mol Toxicol*. 2018;32:e22040. doi:10.1002/jbt.22040
17. Alidadi H, Khorsandi L, Shirani M. Effects of quercetin on tubular cell apoptosis and kidney damage in rats induced by titanium dioxide nanoparticles. *Malays J Med Sci*. 2018;25(2):72–81.
18. Song B, Liu J, Feng X, Wei L, Shao L. A review on potential neurotoxicity of titanium dioxide nanoparticles. *Nanoscale Res Lett*. 2015;10(1):1042. doi:10.1186/s11671-015-1042-9
19. Calderón-Garcidueñas L, Reynoso-Robles R, Pérez-Guillé B, Mukherjee PS, Gónzalez-Maciel A. Combustion-derived nanoparticles, the neuroenteric system, cervical vagus, hyperphosphorylated alpha synuclein and tau in young Mexico City residents. *Environ Res*. 2017;159:186–201. doi:10.1016/j.envres.2017.08.008
20. Choi HS, Ashitate Y, Lee JH, et al. Rapid translocation of nanoparticles from the lung airspaces to the body. *Nat Biotechnol*. 2010;28(12):1300–1303. doi:10.1038/nbt.1696
21. Liu V, Sui B, Sun J. Size- and shape-dependent effects of titanium dioxide nanoparticles on the permeabilization of the blood–brain barrier. *J Mater Chem B*. 2017;5:9558. doi:10.1039/C7TB01314K

22. Oberdörster G, Oberdörster E, Oberdörster J. Nanotoxicology: an emerging discipline evolving from studies of ultrafine particles. *Environ Health Perspect*. 2005;113(7):823–839. doi:10.1289/ehp.7339
23. Razani B, Lisanti MP. Caveolins and caveolae: molecular and functional relationships. *Exp Cell Res*. 2001;271(1):36–44. doi:10.1006/excr.2001.5372
24. Boland S, Hussain S, Baeza-Squiban A. Carbon black and titanium dioxide nanoparticles induce distinct molecular mechanisms of toxicity. *Wiley Interdiscip Rev Nanomed Nanobiotechnol*. 2014;6(6):641–652. doi:10.1002/wnan.1302
25. Disdier C, Chalansonnet M, Gagnaire F, et al. Brain inflammation, blood brain barrier dysfunction and neuronal synaptophysin decrease after inhalation exposure to titanium dioxide nano-aerosol in aging rats. *Sci Rep*. 2017;7(1):12196.
26. Grissa I, Guezguez S, Ezzi L, et al. The effect of titanium dioxide nanoparticles on neuroinflammation response in rat brain. *Environ Sci Pollut Res Int*. 2016;23(20):20205–20213. doi:10.1007/s11356-016-7234-8
27. Oleru UG. Respiratory and nonrespiratory morbidity in a titanium oxide paint factory in Nigeria. *Am J Ind Med*. 1987;12(2):173–180. doi:10.1002/ajim.4700120206
28. Gramowski A, Flossdorf J, Bhattacharya K, et al. Nanoparticles induce changes of the electrical activity of neuronal networks on microelectrode array neurochips. *Environ Health Perspect*. 2010;118(10):1363–1369. doi:10.1289/ehp.0901661
29. Ze Y, Sheng L, Zhao X, et al. Neurotoxic characteristics of spatial recognition damage of the hippocampus in mice following subchronic peroral exposure to TiO2 nanoparticles. *J Hazard Mater*. 2014;264:219–229. doi:10.1016/j.jhazmat.2013.10.072
30. Horváth T, Papp A, Kovács D, Kálomista I, Kozma G, Vezér T. Electrophysiological alterations and general toxic signs obtained by subacute administration of titanium dioxide nanoparticles to the airways of rats. *Clin Neurosci*. 2017;70(3–4):127–135.
31. Afaq F, Abidi P, Matin R, Rahman Q. Cytotoxicity, pro-oxidant effects and antioxidant depletion in rat lung alveolar macrophages exposed to ultrafine titanium dioxide. *J Appl Toxicol*. 1998;18(5):307–312. doi:10.1002/(SICI)1099-1263(1998090)18:5<307::AID-JAT508>3.0.CO;2-K
32. He Q, Zhou X, Liu Y, et al. Titanium dioxide nanoparticles induce mouse hippocampal neuron apoptosis via oxidative stress- and calcium imbalance-mediated endoplasmic reticulum stress. *Environ Toxicol Pharmacol*. 2018;63:6–15. doi:10.1016/j.etap.2018.08.003
33. Coccini T, Grandi S, Lonati D, Locatelli C, De Simone U. Comparative cellular toxicity of titanium dioxide nanoparticles on human astrocyte and neuronal cells after acute and prolonged exposure. *Neurotoxicology*. 2015;48(48):77–89. doi:10.1016/j.neuro.2015.03.006
34. Valdiglesias V, Costa C, Sharma V, et al. Comparative study on effects of two different types of titanium dioxide nanoparticles on human neuronal cells. *Food Chem Toxicol*. 2013;57:352–361. doi:10.1016/j.fct.2013.04.010
35. Rajamanickam G, Narendhiran S, Muthu SP, Mukhopadhyay S, Perumalsamy R. Hydrothermally derived nanoporous titanium dioxide nanorods/nanoparticles and their influence in dye-sensitized solar cell as a photoanode. *Chem Phys Lett*. 2017;689:19–25. doi:10.1016/j.cplett.2017.09.044
36. Wang Q, Huang JY, Li HQ, et al. TiO2 nanotube platforms for smart drug delivery: a review. *Int J Nanomed*. 2016;11:4819–4834. doi:10.2147/IJN.S108847
37. Wang Y, Yao C, Ding L, et al. Enhancement of the immune function by titanium dioxide nanorods and their application in cancer immunotherapy. *J Biomed Nanotechnol*. 2017;13(4):367–380.
38. Kulkarni M, Mazare A, Gongadze E, et al. Titanium nanostructures for biomedical applications. *Nanotechnology*. 2015;26(6):062002. doi:10.1088/0957-4484/26/6/062002
39. Su EP, Justin DF, Pratt CR, et al. Effects of titanium nanotubes on the osseointegration, cell differentiation, mineralisation and antibacterial properties of orthopaedic implant surfaces. *Bone Joint J*. 2018;100-B(1_Supple_A):9–16. doi:10.1302/0301-620X.100B1.BJJ-2017-0551.R1
40. Madarász D, Szenti I, Sápi A, Halász J, Kukovecz A, Kónya Z. Exploiting the ion-exchange ability of titanate nanotubes in a model water softening process. *Chem Phys Lett*. 2014;591:161–165. doi:10.1016/j.cplett.2013.11.021
41. Sayes CM, Wahi R, Kurian PA, et al. Correlating nanoscale titania structure with toxicity: a cytotoxicity and inflammatory response study with human dermal fibroblasts and human lung epithelial cells. *Toxicol Sci*. 2006;92(1):174–185. doi:10.1093/toxsci/kfj197
42. Oszlánczi G, Horváth E, Szabó A, et al. Subacute exposure of rats by metal oxide nanoparticles through the airways: general toxicity and neuro-functional effects. *Acta Biol Szeged*. 2010;54(2):165–170.
43. Koblin DD. Urethane: help or hindrance? *Anesth Analg*. 2002;94(2):241–242.
44. Zandieh S, Hopf R, Redl H, Schlag MG. The effect of ketamine/xylazine anesthesia on sensory and motor evoked potentials in the rat. *Spinal Cord*. 2003;41(1):16–22. doi:10.1038/sj.sc.3101400
45. Zilles K. *The Cortex of the Rat. A Stereotaxic Atlas*. Berlin: Springer; 1984.
46. Kandel ER, Schwartz JH, eds. *Principles of Neural Science*. New York: Elsevier; 1985:643–644.
47. Dési I, Nagymajtényi L. Electrophysiological biomarkers of an organophosphorous pesticide, dichlorvos. *Toxicol Lett*. 1999;107(1–3):55–64. doi:10.1016/S0378-4274(99)00031-4
48. Papp A, Vezér T, Institóris L. An attempt to interpret the fatigue of the somatosensory cortical evoked potential during a stimulus train as a possible biomarker of neurotoxic exposure. *Centre Eur J Occup Environ Med*. 2001;7(3–4):276–281.
49. Horváth T, Vezér T, Kozma G, Papp A. Functional neurotoxicity and tissue metal levels in rats exposed subacutely to titanium dioxide nanoparticles via the airways. *Clin Neurosci*. 2018;71(1–2):35–42.
50. Scimeca M, Bischetti S, Lamsira HK, Bonfiglio R, Bonanno E. Energy Dispersive X-ray (EDX) microanalysis: a powerful tool in biomedical research and diagnosis. *Eur J Histochem*. 2018;62:2841.
51. National Institute for Occupational Safety and Health (NIOSH). Current intelligence bulletin 63: occupational exposure to titanium dioxide. NIOSH publication No. 2011–160. 2011
52. Baisch BL, Corson NM, Wade-Mercer P, et al. Equivalent titanium dioxide nanoparticle deposition by intratracheal instillation and whole body inhalation: the effect of dose rate on acute respiratory tract inflammation. *Part Fibre Toxicol*. 2014;11:5. doi:10.1186/1743-8977-11-5
53. Oyabu T, Morimoto Y, Hirohashi M, et al. Dose-dependent pulmonary response of well-dispersed titanium dioxide nanoparticles following intratracheal instillation. *J Nanoparticle Res*. 2013;15(4):1600–1610. doi:10.1007/s11051-013-1600-y
54. Sun Q, Tan D, Ze Y, et al. Pulmotoxicological effects caused by long-term titanium dioxide nanoparticles exposure in mice. *J Hazard Mater*. 2012;235–236:47–53. doi:10.1016/j.jhazmat.2012.05.072
55. Morgan A, Galal MK, Ogaly HA, Ibrahim MA, Abd-Elsalam RM, Noshy P. Tiron ameliorates oxidative stress and inflammation in titanium dioxide nanoparticles induced nephrotoxicity of male rats. *Biomed Pharmacother*. 2017;93:779–787. doi:10.1016/j.biopha.2017.07.006
56. Hanot-Roy M, Tubeuf E, Guilbert A, et al. Oxidative stress pathways involved in cytotoxicity and genotoxicity of titanium dioxide (TiO2) nanoparticles on cells constitutive of alveolo-capillary barrier in vitro. *Toxicol in Vitro*. 2016;33:125–135. doi:10.1016/j.tiv.2016.01.013
57. Huerta-García E, Pérez-Arizti JA, Márquez-Ramírez SG, et al. Titanium dioxide nanoparticles induce strong oxidative stress and mitochondrial damage in glial cells. *Free Rad Biol Med*. 2014;73:84–94. doi:10.1016/j.freeradbiomed.2014.04.026

58. Bhargava P, Schnellmann RG. Mitochondrial energetics in the kidney. *Nat Rev Nephrol*. 2017;13(10):629–646.
59. Boengler K, Kosiol M, Mayr M, Schulz R, Rohrbach S. Mitochondria and ageing: role in heart, skeletal muscle and adipose tissue. *J Cachexia Sarcopenia Muscle*. 2017;8:349–369.
60. Mandal A, Drerup CM. Axonal transport and mitochondrial function in neurons. *Front Cell Neurosci*. 2019;13:373. doi:10.3389/fncel.2019.00373
61. Wilson CL, Natarajan V, Hayward SL, Khalimonchuk O, Kidambi S. Mitochondrial dysfunction and loss of glutamate uptake in primary astrocytes exposed to titanium dioxide nanoparticles. *Nanoscale*. 2015;7(44):18477–18488. doi:10.1039/C5NR03646A
62. Nalika N, Parvez S. Mitochondrial dysfunction in titanium dioxide nanoparticle-induced neurotoxicity. *Toxicol Mech Meth*. 2015;25(5):355–363. doi:10.3109/15376516.2015.1020183
63. Meena R, Paulraj R. Oxidative stress mediated cytotoxicity of TiO 2 nano anatase in liver and kidney of Wistar rat. *Toxicol Environ Chem*. 2018;100-B(1_Supple_A):146–163. doi:10.1080/02772248.2011.638441
64. Koltermann-Jülly J, Keller JG, Vennemannd A, et al. Abiotic dissolution rates of 24 (nano)forms of 6 substances compared to macrophage-assisted dissolution and *in vivo* pulmonary clearance: grouping by biodissolution and transformation. *NanoImpact*. 2018;12:29–41. doi:10.1016/j.impact.2018.08.005
65. Singh A, Kukreti R, Saso L, Kukreti S. Oxidative stress: a key modulator in neurodegenerative diseases. *Molecules*. 2019;24:1583. doi:10.3390/molecules24081583
66. Sárközi K, Nagy V, Papp A, Tombácz E, Szabó A. The effect of three natural antioxidants on the general and nervous system toxicity of manganese nanoparticles in rats. *Centre Eur J Occup Environ Health*. 2013;19(1–4):31–42.
67. Coulter DA, Eid T. Astrocytic regulation of glutamate homeostasis in epilepsy. *Glia*. 2012;60(8):1215–1226. doi:10.1002/glia.22341
68. Héja L, Nyitrai G, Kékesi O, et al. Astrocytes convert network excitation to tonic inhibition of neurons. *BMC Biol*. 2012;10:26. doi:10.1186/1741-7007-10-26
69. Takahashi M, Billups B, Rossi D, Sarantis M, Hamann M, Attwell D. The role of glutamate transporters in glutamate homeostasis in the brain. *J Exp Biol*. 1997;200(Pt 2):401–409.
70. Kreitzer AC, Malenka RC. Striatal plasticity and basal ganglia circuit function. *Neuron*. 2008;60(4):543–554. doi:10.1016/j.neuron.2008.11.005
71. Horváth T, Szabó A, Lukács A, et al. Investigation of subacute neurotoxicity of titanium-dioxide nanoparticles in rat model. *Egészségtudomány*. 2016;60(4):7–23.
72. Smith SJ, Harding AE. EEG and evoked potential findings in mitochondrial myopathies. *J Neurol*. 1993;240(6):367–372. doi:10.1007/BF00839969
73. Metherate R, Cox CL, Ashe JH. Cellular bases of neocortical activation: modulation of neural oscillations by the nucleus basalis and endogenous acetylcholine. *J Neurosci*. 1992;12(12):4701–4711. doi:10.1523/JNEUROSCI.12-12-04701.1992
74. Hegerl U, Juckel G, Möller HJ. Event related brain potentials as indicators of neurochemical dysfunctions in psychiatric patients. *Nervenarzt*. 1996;67(5):360–368.
75. Iadecola C, Gottesman R. Neurovascular and cognitive dysfunction in hypertension: epidemiology, pathobiology and treatment. *Circ Res*. 2019;124(7):1025–1044. doi:10.1161/CIRCRESAHA.118.313260
76. Calderón-Garciduenas L, González-Maciel A, Reynoso-Robles R, et al. Quadruple abnormal protein aggregates in brainstem pathology and exogenous metal-rich magnetic nanoparticles (and engineered Ti-rich nanorods). The substantia nigrae is a very early target in young urbanites and the gastrointestinal tract a key brainstem portal. *Environ Res*. 2020;191:110139.